Faculty of Science

Land Use and Land Cover Changes in Europe and the Impact on Near-Surface Wind Speed in Sweden

Nils Philipp Stange

Degree of Master of Science (120 credits)
with a major in Atmosphere, Climate and Ecosystems
60 hec

Department of Earth Sciences
University of Gothenburg
2023 B1259

UNIVERSITY OF GOTHENBURG

UNIVERSITY OF GOTHENBURG
Department of Earth Sciences
Geovetarcentrum/Earth Science Centre

Land Use and Land Cover Changes in Europe and the Impact on Near-Surface Wind Speed in Sweden

Nils Philipp Stange

ISSN 1400-3821

B1259
Master of Science (120 credits) thesis
Göteborg 2023

Mailing address	Address	Telephone	
Geovetarcentrum	Geovetarcentrum	031-786 19 56	Geovetarcentrum
S 405 30 Göteborg	Guldhedsgatan 5A		Göteborg University
			S-405 30 Göteborg
			SWEDEN

Abstract

Investigations of Land use and land cover change (LULCC) have recently become of increasing interest. This trend occurs not only based of the importance of biogeochemical processes such as carbon sequestration, but also because of their climate impacts caused by changed biogeophysical properties. This study examines the LULCC in Europe between 2000 and 2018 based on the Corine Land Cover raster maps created by Copernicus, with a focus on Sweden and the impact on near-surface wind speed. For this purpose, 59 wind stations in Sweden were selected where changes within a radius of 1 km have been found. These LULCC were classified, and appropriate surface roughness values were assigned based on existing literature. Using a geographic information system, the surface roughness changes were then characterized and documented. With the help of an ODR-method (Observation divided by Reanalysis), this study tried to utilize the inherent properties of ground-based observations and reanalysis data (ERA5) to find out if near-surface wind speed changes are a result of LULCC. The analysis shows strong decreases in Agricultural land across Europe, which is partly replaced by Urban areas at the outskirts of metropolitan areas as well as forest areas. Furthermore, no clear correlations between LULCC and the near-surface wind speed are apparent, which indicates that the wind speed is not strongly affected by the local changes in Land use and land cover (LULC). Errors in the raster data of LULC may also play a role in masking the relationship between changed surface roughness and wind speed.

Sammanfattning

Undersökningar av förändringar i markanvändning och marktäcke har på senare tid blivit alltmer intressanta. Denna trend beror inte bara på biogeokemiska processer, t.ex. kolbindning, utan också på frågor om deras biogeofysiska egenskaper som har dykt upp. I den här studien undersöks förändringarna i markanvändning och marktäckning i Europa mellan 2000 och 2018 utifrån Corine Land Cover rasterkartor som skapats av Copernicus. Ytterligare fokus ligger på att undersöka förhållandet mellan dessa förändringar med fokus på Sverige och deras inverkan på vindhastigheten nära ytan. För detta ändamål valdes 59 vindstationer i Sverige ut där förändringar hittades inom en radie av 1 km. Förändringarna i markanvändning och marktäcke undersöktes och lämpliga värden för ytjämnhet tilldelades utifrån befintlig litteratur. Med hjälp av ett geografiskt informationssystem identifierades och dokumenterades förändringarna i ytjämnhet. ODR-metoden (Observation divided by Reanalysis) användes för att utnyttja de inneboende egenskaperna hos markbaserade observationer och reanalysdata (ERA5) för att ta reda på om förändringar i vindhastigheten nära ytan är ett resultat av förändringar i markanvändning och marktäcke. Analysen visar en kraftig minskning av jordbruksmark i hela Europa, som delvis ersätts av stadsområden i utkanten av storstadsområden och av skogsområden. Dessutom finns inga tydliga korrelationer mellan förändringar i markanvändning och marktäcke och vindhastigheten nära ytan, vilket tyder på att vindhastigheten inte påverkas starkt av de lokala förändringarna i markanvändning och marktäcke. Fel i rasterdata för LULC kan också spela en roll när det gäller att dölja sambandet mellan förändrad ytjämnhet och vindhastighet.

Acknowledgments

I would like to express my deep gratitude to my supervisor Deliang Chen for all his trust and advice along the way. This thesis would not have been possible without his support and guidance. The same applies to my Co-Supervisor Gustav Strandberg, whose valuable ideas and input were significant to this project. I would furthermore like to thank my examiner Fredrik Lindberg for his much appreciated feedback on this thesis. I would be remiss if I did not thank Tinghai Ou, Alexander Walther, Julia Kukulies and Cheng Shen for always having an open ear when I needed technical support or had questions regarding data processing.

A tremendous thank you goes to my dear family, who has supported me from day one and continued to do so during the past six years of my academic career regardless of the geographical situation. I would not be here without any of you. Finally, and most importantly, I would like to thank my beloved Isi for her perpetual encouragement and relentless support. It means the world to me.

Contents

List of Tables

List of Figures

Acronyms

ABL Atmospheric boundary layer

CLC Copernicus land cover

ERA5 ECMWF reanalysis v5

IPCC Intergovernmental panel on climate change

LAI Leaf area index

LC Land cover

LCC Land cover change

LU Land use

LUC Land use change

LULC Land use and land cover

LULCC Land use and land cover change

NSWS Near-surface wind speed

ODR Observation divided by reanalysis

PGF Pressure-gradient force

SMHI Swedish meteorological and hydrological institute

SR Surface roughness length

SRC Surface roughness length change

Nomenclature

ha Hectar

$\mathbf{km^2}$ Square kilometer

m Meter

$\mathbf{m\ s^{-1}}$ Meter per second

p Statistical p-value

$\mathbf{r_x}$ Correlation of surface roughness change and Near-surface wind speed

z Height above ground

$\mathbf{z_0}$ Roughness parameter

$\vec{F}$ Coriolis effect

$\vec{f}$ Drag force

$\vec{G}$ Pressure-Gradient force

$\vec{g}$ Gravitational force

$\vec{U}_\mathbf{x}$ Wind speed

u^* Friction velocity

$\vec{u}$ Horizontal component of the wind

$\vec{v}$ Vertical component of the wind

κ Von-Karman constant

$\vec{\Omega}$ Angular velocity

ϕ Degree wind direction

1 Introduction

Since the introduction of the industrial revolution the global climate has effectively changed. These changes have been intensified during the 20^{th} century and continued during the first two decades of the 21st century. In fact, tremendous consensus exists among the scientific community that these changes not only occurred, but that they are also strongly influenced by anthropogenic processes [Masson-Delmotte et al. (2021)] The Working Group 1 of the Intergovernmental panel on climate change (IPCC) summarized the scientific findings famously in their most recent publication, the "Assessment Report 6 - The Physical Science Basis. Therein, it states:

> "It is unequivocal that human influence has warmed the atmosphere, ocean and land. Widespread and rapid changes in the atmosphere, ocean, cryosphere and biosphere have occurred." [Masson-Delmotte et al. (2021)]

One of the biggest anthropogenic sources of radiative forcing is the alteration of LULC. Its tremendous significance shows in its contribution, of about one-third of all emissions, since the beginning of the industrialization [Devasthale et al. (2022)]. This process, most often referred to as LULCC, can alter our climate in different ways. LULCC has an impact on climate through two different processes or mechanisms, the biochemical and the biophysical process. A brief description on these two mechanisms can be found in Section 1.1.1 and 1.1.2 respectively. During the past decades, the biochemical processes have been extensively examined. A broad field of knowledge has been established in that regard. At the same time, broad research on biophysical processes started to intensify in the 2010s. These mechanisms and the understanding for them are of utmost importance because of their vast impact on the global and regional climate. Although high confidence in the premise of the biophysical effects exists, medium confidence about the sign and the magnitude of the net effect persists globally [Jia et al. (2019)].

1.1 Distinction between land use and land cover

Land cover (LC) describes the biophysical attributes of the earth's surface [Lambin et al. (2001)], i.e. the vegetation, structure or system that covers a land area. That can apply to urban areas, forests or agricultural areas. A multitude of LC classes and types exist depending on how detailed one might look at it. Changes of the LC will most often lead to changes of the biochemical and biophysical response as photosynthesis and respiration increase or decrease, species and their ecosystem are redistributed or disappear entirely and finally the function and structure of the previous LC will be altered [Jia et al. (2019)]. As a result of Land cover change (LCC) and the subsequent alteration of the biochemical and biophysical mechanisms, the climate experiences local, regional and global changes, whose scale depends on the dimensions of the LCC.

Land use (LU) describes the intention or purpose humans have for a certain LC [Lambin et al. (2001)], meaning how certain LC types are managed, e.g. whether arable land is being irrigated, fertilizers of different types are applied or what species of trees a forest consists of. LU is often a result of the environment, meaning certain regions experience a background climate that forces the landowner to implement certain land management practices in order to increase the productivity or to ensure certain living conditions for the LC. The type of land management can impact the regional climate by altering the biogeochemical feedback when the LC is stimulated with a surplus of water or nutrients, leading to quicker and higher growth rates or as a result of lacking management causes the LC to experience a growth deficiency [Hirsch et al. (2017)]. It can also impact the biogeophysical feedback, altering the albedo, evaporation rates and surface roughness, by choosing different crop or vegetation types. A more detailed description of the implications of LULCC on the biochemical and biophysical processes can be found in Section 1.1.1 and 1.1.2 respectively. Both, LC and LU can be influenced anthropologically, but the premise is that LCC will automatically change the LU type. That does, however, not apply the other way around.

1.1.1 Biogeochemical processes

Biogeochemical processes, that result in radiative forcing, include the release and uptake of greenhouse gases, primarily carbon dioxide. The gases can either be stored in sinks, e.g. in the oceans, the atmosphere and the biosphere or they occur as fluxes that move in between theses sinks. These processes can be summarized as the so-called carbon cycle. While by no means the most import sink, the land carbon dioxide uptake is driven by the vegetation. Natural interannual variability in its CO_2-uptake exists, e.g. due to the El Niño-Southern Oscillation [Masson-Delmotte et al. (2021)], but changes of the LULC can enhance this variability by altering the carbon stocks [Lejeune et al. (2018)]. Despite vast importance of the biogeochemical processes for our climate, this study will focus on the biogeophysical processes, particularly changes of the Surface roughness length (SR) because of its importance for the wind speed (see Section 1.1.2 and 1.2).

1.1.2 Biogeophysical processes

Biogeophysical processes occur as a result of the inherent properties of the land cover. Generally, one can assume that these processes have a more immediate and localized impact compared to biochemical processes [Jia et al. (2019)]. Despite strong signals locally, LULCC induced alteration of biophysical processes leads to rather small signals globally [Alkama et al. (2016)]. The three most prominent mechanisms are the Albedo, the Evapotranspiration and the SR.

1. The planetary albedo [α_p] refers to the fraction of solar energy that is being scattered back from the Earth's surface [Stephens et al. (2015)]. It is approximated at an average of 29% but differs considerably depending on the surface. Especially for terrain where the land cover is heterogeneous, the value of the albedo may change on extremely small scales. How much shortwave radiation is scattered back or emitted as longwave radiation is directly and inherently dependent on the properties of the surface and land cover. This is an important mechanism because changes thereof can alter the energy distribution between land and atmosphere and thus influence potentially other mechanisms, such as the Pressure-gradient force (PGF), the hydrological cycle (including the sensible and latent heat flux) as well as the vegetation dynamics [Bright et al. (2015)].

2. Depending on the species, the partitioning of net radiation into the latent and sensible heat fluxes may differ in boreal forests. While deciduous broad-leaf tree species show high rates of sensible heat flux, which results in a deep Atmospheric boundary layer (ABL), coniferous species have a low ratio of latent heat flux to available energy [Bonan et al. (2008)]. This can be essential because of the ABL's role in the development of wind. Section 1.2 will pick up on that.

3. The most important parameter for the Near-surface wind speed (NSWS) is the SR and potential changes therein. Vegetation, relief and other artificial obstacles alter the aerodynamic

roughness characteristics that the mean surface wind flow will encounter. The higher and denser the obstacle, the more it alters the mean wind speed [Troen & Petersen (1989)], direction and vertical wind shear [Oke (1987)]. The surface roughness is indicated by the roughness parameter z_0, which is chosen so that the wind velocity $\vec{U}(z_0) = 0$. It is an experimentally determined constant [Sorbjan (1989)] and changes depending on the characteristics of the surface. Those include the shape, density and flexibility of the surface and/or obstacles [Oke (1987)]. For forests specifically, z_0 is a function of Leaf area index (LAI) and the canopy height [Bright et al. (2015)]. A more detailed description of its influence on wind is provided in Section 1.2.

1.2 Theory of near-surface wind speed

Wind has vast impacts on daily human life. It can provide electrical energy through wind power plants, and serve vegetation as a pollen transport [Minola et al. (2022)], but it also has important functions moving and distributing heat and water through the atmosphere and thus contributes to the hydrological cycle and heat exchange through evapotranspiration [McVicar et al. (2012)]. On contrast, wind is responsible for damages to human life and infrastructure as well as natural land cover change due to wind gusts or turbulences. These turbulences can in turn be enhanced or weakened by changes in the SR. It is important to understand the effect of Surface roughness length change (SRC) on the NSWS. The following section will show the principle that wind is based on, but it is important to mention upfront that it is a simplification of the atmospheric processes.

$$\frac{d\vec{U}}{dt} = \vec{G} + \vec{F} + \vec{g} + \vec{f} \tag{1}$$

Wind can be described as a motion in the atmosphere, which is described by the Lagrangian form of the wind equation 1, where $d\vec{U}\ dt^{-1}$ describes the wind speed over time, $\vec{G}$ describes the PGF, $\vec{F}$ is the Coriolis force: $\vec{F}$ = -2$\vec{\Omega} \times \vec{U}$, $\vec{g}$ is the gravitational force and $\vec{f}$ describes the drag force [Wu et al. (2018)].

Equation 1 suggests, that because the Coriolis force is passive and the gravitational force is almost constant, the wind speed changes can mainly be attributed to the alteration of the PGF or the drag force [Wu et al. (2018)]. The PGF is a result of thermal energy input, i.e. heating the surface with varying magnitude in different locations and causing an unequal rise of air masses and consequently deviating pressure differentials. It is thus a driving force. The drag force, on the contrary, can decelerate the wind. One has to distinguish between the external and internal friction making up the drag force. The internal friction is due to changes in the atmospheric boundary layer conditions, e.g. static stability, vertical momentum transport, local circulation and the vertical wind shear. The external friction can mainly be attributed to the changes in LULC [Wu et al. (2018)]. Assuming a constant PGF, the wind speed will differ at a constant height if it is affected by different magnitudes of drag force. With this assumption in mind, one can describe the wind velocity as a function of height z and the friction velocity u*:

$$\vec{U}(z) - \vec{U}(z_0) = \frac{u^*}{\kappa} * ln(\frac{z}{z_0}) \tag{2}$$

Equation 2 suggests, that the wind profile at the height z is scaled by the surface roughness z_0 as well as that the wind velocity $\vec{U}$ is depending on the friction velocity u* and the dimensionless von-Karman constant κ [Sorbjan (1989)]. The von-Karman constant, measured by Andreas et al. (2006) to be 0.387, puts the wind shear profile in relation to the surface stress. The sum of all wind velocity vectors at z_0 is zero because of the rigidity of the earth. With increasing elevation within the boundary layer, the horizontal wind velocity increases as a function of the course. An important note is that this conjecture is only true as long as we assume the thermal variable to be constant [Sorbjan (1989)] [Oke (1987)]. Because this study investigates the near-surface wind, it is reasonable to assume that z_0 is of vast importance as it affects the wind.

The concept of relative wind speed decrease as a result of obstacles is described as the Shelter effect in the European Wind Atlas [Troen & Petersen (1989)]. Obstacles can be artificial or part of the terrain, but one inherent property is the surface roughness length z_0. Troen & Petersen (1989) show that the strength of the shelter effect is dependent on a few variables: The distance from the obstacle to the site, the height of the obstacle, the height of the point of interest, the length of the obstacle and the porosity/density of the obstacle. This concept will be of importance for this study as it is going to be applied as a rule of thumb for the selection of the wind stations in Section 2.2.

1.3 Implications of land use and land cover changes for Sweden

A quite distinct way of using their national resources can be found in Scandinavia, more specifically in Sweden. Forestry has been an important economic branch for Sweden with 2.2% of the GDP in 2011 [Blanco et al. (2017)]. Between 2017 and 2022 278,720 km^2 (69%) of the Swedish land was covered by forests, with an additional 52,840 km^2 (6%) covered in so-called "*Other wooded land*" that includes trees and shrubs [Nilsson et al. (2022)]. Since the beginning of the 20^{th} century, the Swedish surface area has been increasingly forested, with the peak of forestation rates in the 1960s. In 2018, Sweden practiced forest felling at the standing age of approximately 100 years, but since the year 2004 the felling age has declined on average 20 years, depending on the region [Nilsson et al. (2022)]. Blanco et al. (2017) conclude that this will result in a supply peak in the 2030s lasting into the 2050s, although they add that the magnitude of the peak is dependent on logistical and economic variables. Assuming the climatic variables are as easily influenced by altered biophysical parameters due to LULCC, as described by [Lejeune et al. (2018)], this scenario might have major implications for Sweden's, but also Europe's climate. Subsequently, it is vital to examine what LULCC has looked like in Europe and whether climate variables changed in the past and if they correlate to LULCC regionally. A number of studies have already been conducted, examining the effect of LULCC on the climatic variables. Most studies focused on the impact on the near-surface or surface temperature in boreal regions ([Alkama et al. (2016)], [Arora & Montenegro et al. (2011)], [Bright et al. (2017)], [Davin et al. (2020)], [Devaraju et al. (2018)], [Liao et al. (2020)], [Sofiadis et al. (2022)], [Strandberg et al. (2019)] and [Tölle et al. (2018)]), in temperate regions ([Ahlswede et al. (2017)], [Alkama et al. (2016)], [Arora & Montenegro et al. (2011)], [Boisier et al. (2012)], [Bright et al. (2017)], [Davin et al. (2020)], [Devaraju et al. (2018)], [Liao et al. (2018)], [Liao et al. (2020)], [Luyssaert et al. (2014)], [Sofiadis et al. (2022)], (2019)] and [Tölle et al. (2018)]) and in tropical regions ([Alkama et al. (2016)], [Arora & Montenegro et al. (2011)], [Bright et al. (2017)], [Cohn et al. (2019)], [Davin et al. (2020)], [Devaraju et al. (2018)], [Liao et al. (2020)] and [Zeng et al. (2021)]).

To date, comparatively few studies have looked at the impact of LULCC on the NSWS. Using numerical modeling, Zha et al. (2019) found that a NSWS slowdown over China could mainly be attributed to increased SR. Two additional studies tried to quantify the impact of terrestrial LULCC and consequently SRC on near-surface wind speed. Wever (2012) explored 157 wind station in Europe for 1981–2009 and found that approximately 70% of the wind speed trend can be attributed towards SRC. The study lacks, however, real LULC observations. In his paper, Wever (2012) estimates the local roughness length from the wind speed observations. Vautard et al. (2010) propose that 25-60% of the wind speed changes can be attributed to SRC in the Northern Hemisphere. To indicate the LULC in their study, they use observational wind data from 822 stations in North America and Eurasia. They additionally used ERA-Interim data sets at a coarse resolution of 2.5° to complement their wind data. *Normalized Difference Vegetation Index* provided by the *Global Agricultural Monitoring System* with a medium resolution of 8 km was used as their SR indicator. At the same time, no regular observations of the impact of surface roughness or the surface drag force had been made [Wu et al. (2018)]. Minola et al. (2022) initiated to tackle this question. Using high resolution LULC data as the explanatory variable in a linear regression with NSWS in between the time period 1998-2018, they found the regression to be $R^2 = 0.53$, after removal of outliers. The sample size of wind stations for the investigation of LULCC was, with n = 13, rather small. Additionally, the study is based solely on observational station data. Finally, Luu et al. (2023) tried to simulate the effect of LULCC on the NSWS in western Europe using the LUCAS-LUC database for the LULC as well as ECMWF reanalysis v5 (ERA5) and the E-OBS gridded observation database for the NSWS. They found changes of the mean and maximum NSWS to be partly a result of large scale circulation changes and partly of the changes in SRC. However, they emphasize that the LUCAS-LUC database contains uncertainties due to derivations from reconstructions, especially compared to currently available satellite data.

1.4 Objectives

Despite the large number of studies on the matter, to date almost no high resolution quantification of the observed LULCC in Europe has been conducted. Only Zhou et al. (2021) investigated the LCC in the Nordic countries between 1992 and 2018 using two LC products of 300 meter resolution. In order to understand the impact of past changes onto the climate, one ought to overcome the lack of observed LULCC for the European continent. It is therefore necessary to extent the already existing work by quantifying the LULCC in Europe and projecting their induced effect on the SR, continuing with a quantification of SRC impact on the NSWS from observations. As a result of the scarcity of research on past LULCC in Europe and its subsequent impact on near-surface wind, this study has two main objectives:

1. Compile and map LULCC in Europe at high resolution to improve the lacking understanding of the changes in the recent past (2000-2018) and subsequently focus on the surface roughness in Sweden.

2. Analyze the observed NSWS changes over Sweden in regard to the LULCC/SRC found in objective one. For this purpose, the work of Minola et al. (2022) will be extended by introducing a larger sample size, isolating the effect of the SRC using the Observation divided by reanalysis (ODR)-method and finally distinguishing between changes on a directional level. More information on the ODR-method will be given in Section 2.2.4.

2 Data and methodology

This section will proceed to describe the decision-making process, i.e. why the respective data sets and methods in this study were used to achieve the above mentioned objectives. It will first introduce the LULC data set and then follow up with the data sets of the near-surface wind and the description of the ODR-method.

2.1 Data on land use change

For objective number one, the LULC data that is used in this study was downloaded from the Copernicus Land Monitoring Service web page (2023). The Copernicus land cover (CLC) maps are prepared using remote sensing satellite data. The spatial resolution of the CLC vector layer maps is 100 meter, but a minimal mapping unit of 25 hectare was set. That means, the CLC product carries no vectors and classes under 25 hectare, respectively. The raster layer is then created by "rasterization" of the vector layer, using the ArcGIS *Cell Center Method* [Büttner et al. (2021)]. With this method a raster grid is created and the center point within each raster is considered the majority class in the respective cell. The authors name a "Thematic accuracy" of $\geq$ 85% for the vector layer, but no information is provided for the raster layer [Kosztra et al. (2019)]. For a deeper technical description of the CLC product consider the Product User Manual, provided by Copernicus Land Monitoring Service [Büttner et al. (2021)]. The CLC product consists of 44 different LULC classes and one *No Data* class. To get a more coherent and clear picture of the LULC in Europe, the classes were naturally grouped according to their LU and furthermore, a second grouping was conducted according to their SR. To assist the process of LULC-grouping, the "Updated CLC illustrated nomenclature guidelines" created by the European Environment Agency were taken into consideration [Kosztra et al. (2019)]. The 45 original classes are shown in Table 7. This study will use the group "Shrub & transitional Woodland", from the above-mentioned Table, to identify areas of deforestation and forestation. The reason is that the CLC *Transitional woodland/shrub* is described as: "Areas representing natural development of forest formations, consisting of young plants of broad–leaved and coniferous species, with herbaceous vegetation and dispersed solitary adult trees. Transitional processes can be for instance natural succession on abandoned agricultural land, regeneration of forest after damages of various origins (e.g. storm, avalanche), stages of forest degeneration caused by natural or anthropogenic stress factors (e.g. drought, pollution), reforestation after clear-cutting, afforestation on formerly non-forested natural or semi-natural areas etc." [Kosztra et al. (2019)]. Kosztra et al. (2019) suggest that it is thus applicable for the intended clear-cut forest areas, thinned areas, selective cuts and areas that experienced harsh environmental conditions like heat stress, pollution or storms. These areas are, as the name suggests, in transition and are likely to change their state of LULC within a few years, due to natural succession. Because this study groups this class together with the class *Sclerophyllous vegetation*, it should be considered with care, especially in the Mediterranean region. In northern Europe and more specifically the boreal regions like Sweden, this should work well as an indicator due to the lack of Sclerophyllous vegetation. Finally, the grouping by surface roughness was done with the help of Silva et al. (2007), who ascribed surface roughness values according to CLC nomenclature. Because no class resembles another class exactly a certain leeway was given to fit the classes. The SR-specific values for each CLC category are displayed in Table 7, including the minimum, maximum and most likely SR.

As mentioned above, the time span, considered in this study, is CLC 2000 until CLC 2018. Copernicus does offer LULC maps dating back until the year 1990. However, until the year 2000, no CLC maps had included a visual representation of Sweden's territory. Therefore, the time frame of 2000 until 2018 had to be chosen for this study. Of interest was not the LULC per se, but rather the change in between the study period (2000-2018). To quantify the changes, the geographic information systems *QGIS* and *ArcMap* were utilized. The CLC 2000, 2006, 2012 and 2018 maps were regrouped in *QGIS* according to Table 7 and were given a distinct value. With the help of the Raster Calculator, a very simple procedure was conducted.

$$LULCC = CLC_{new} – CLC_{old} \tag{3}$$

This procedure was conducted for the time span 2000–2018, in order to understand where LULCC occurred, as well as every time step in between (2000–2006, 2006–2012 & 2012–2018) to understand when certain changes were induced. A rough visual inspection of larger changes was conducted and changes were dismissed, if the change are likely to be a result of subjectivity and therefore negligible. Two primary changes were thus neglected:

1. Any transitions from the classification of *forest* to *Coniferous forest* and vice versa cannot with certainty be labeled as a change because of the arbitrary definition of *Mixed forests*. According to the nomenclature, a Mixed forest includes areas with "evergreen or deciduous coniferous (needle-leaved) trees with 25-75%" of the total crown cover. The Coniferous forest class includes "evergreen and deciduous coniferous trees species [...] with $\geq$ 75% share" of the total crown cover. It is quiet apparent, that the precise ratio of coniferous to deciduous tree species is not determinable. To exaggerate this example, the proclaimed change could thus be as vast as 25% $\rightarrow$ 100% coniferous tree species, or for instance, it could be as marginal of a change from 72% $\rightarrow$ 76%.

2. Any transition from *Grassland & Heathland* to *Marshes & Peatbogs* and vice versa wasn't considered. The reason for this step lies in the similarity of the classes' properties. One could argue that they should be grouped together after all, but in this study they were grouped apart because of the biophysical parameters inferred from S. Hagemann (2002).

After dismissal, changes were quantified using the 'Zonal Histogram' function in QGIS, with the LULCC raster and country-specific zones that were created by Natural Earth (2023) with the scale of 1:10m. For the output maps in Section 3.2 the resolution of the LULCC will be decreased to 5x5 km using the resampling tool and its nearest neighbour method in ArcGIS. This serves the purpose of visibility. However, the numerical documentation, will be conducted using the 100 meter resolution layer. The same procedure was applied for the extraction of the SRC-information, with the difference of the grouping and the ascribed values. For the SRC, Equation 4 was applied.

$$SRC = SR_{new} – SR_{old} \tag{4}$$

According to Equation 4, a negative SRC value implies a decrease in SR and a positive SRC value implies an increase in SR. All of these changes will be described in Section 3. The changes in Europe will be described on a country basis, i.e. each country's changes are quantified independently. Afterwards, a more detailed look at Sweden will be taken. For this purpose, the terrestrial territory of Sweden is divided into 3 major regions: Norrland, Svealand and Götaland. These regions are further subdivided into 21 counties or "Iän".

2.2 Near-surface wind speed observed and simulated by reanalysis

2.2.1 Observations

To tackle the second objective, this study resorts to two different types of wind data sets. The first source of data in this study is observational wind data, more specifically, wind data sets produced by the Swedish meteorological and hydrological institute (2023). The weather stations of the Swedish meteorological and hydrological institute (SMHI) are spread nationwide and the observations of many meteorological stations date back decades. In total, 168 wind stations, spread over the entire Swedish mainland and Öland, were checked for LULCC and SRC, respectively. For a station to pass and to be classified as having experienced sufficiently vast LULCC, it has to show some form of change in a one-kilometer radius. As described in Section 1.2, the shelter effect depends on different variables that vary from site to site. This limit seemed therefore to be reasonable. Ultimately, 59 stations were found to be in the proximity of sufficient LULCC and to have consistently long wind data documentation. These stations were thus left for further processing and examination. They can be found in Table 9.

The observational data is stored in comma-separated value files (.csv). Each station's file includes information about the station name, the station number, the station net, and the measuring height. Furthermore, it contains the start of measurement, the last measurement (to date), the height above sea level as well as the latitude and the longitude. Finally, information about the date (month/day/year), time (hour:minutes:seconds), wind direction and wind speed are included. Both, the direction and velocity are followed by a quality indicator (G and Y), where G stands for green and Y stands for yellow. SMHI describes their purpose as follows: "Green = Checked and approved values. Yellow = Suspicious values, aggregated values, roughly checked archive data and unchecked real-time data (last 2 hours)".

2.2.2 ERA5 reanalysis

The second source of data utilized in this project are ERA5 wind data sets from the Copernicus Climate Change Service [Hersbach et al. (2023)]. More specifically, the data sets include *ERA5 hourly data on single levels from 1940 to the present.* ERA5 is a Reanalysis product that is set up with a grid size of 0.25°, which measures up to approximately 31 km. Reanalysis products combine observations and models, leading to a consistent output of the climate variables on a gridded map without gaps. They can thus provide an accurate representation of the main Earth system cycles, such as the hydrological and energy cycle [Hersbach et al. (2020)]. In ERA5, the land data is assimilated to analyze the land surface prognostic variables, such as the soil texture and the bare soil evaporation using the land surface scheme HTESSEL [Hersbach et al. (2020)]. HTESSEL is a tiled scheme for surface exchanges over land, that incorporates the land surface hydrology and describes the soil, vegetation and snow at different spatial resolutions. It derives among others the SR from the characteristics of the tiles, which is then passed to the atmospheric model [ECMWF (2023a)]. The land cover does not represent urban environments [ECMWF (2023a)], and although it accounts for the seasonally varying vegetation, it does not describe the changes of the LC over time [Hersbach et al. (2020)]. One can therefore assume that the LULC and the SR are fixed and that any changes in wind speed over time can be ascribed to the changes in the driving force.

For this study, the 10 m $\vec{u}$-component of wind variable as well as the 10 m $\vec{v}$-component of wind variable were chosen for the same time period as the observational data (1996-2021). By employing

Equation 5 shown by the European Centre for Medium-Range Weather Forecasts (2023b), the degree wind direction ϕ can be determined from the $\vec{u}$-component and $\vec{v}$-component of the wind vector. Similarly, one can extract the wind speed by employing Equation 6 shown by Quesada et al. (2017).

$$\phi = mod(180 + \frac{180}{\pi} atan2(\vec{v}, \vec{u}), 360) \tag{5}$$

$$|\vec{U}| = \sqrt{\vec{u}^2 + \vec{v}^2} \tag{6}$$

Because the ERA5 data is based both longitudinally and latitudinal on grid points of 0.25 degrees, 59 grid points were isolated that corresponded best to each wind station, i.e. that were located closest. The time series of these isolated grid points were then indexed from the data set and implemented into the SMHI data sets of the corresponding station. The Reanalysis data sets serve two main purposes.

1. The ERA5 data sets contain information about the direction vectors and have the advantage of showing the prevailing wind direction. The observational data detects the wind direction too, but as a result of the influence of natural barriers, the true wind direction could be altered. One example is a wind draft that comes from the north but is deflected by a river valley that runs along the east-west axis, resulting in a detection of non-north wind. By utilizing the prevailing wind direction, this study intends to mitigate this mistake and show the true impact that LULCC has on the NSWS.

2. The influence of the LULC in ERA5 is set to be constant and thus enables for this study to employ the ODR method [Wu et al. (2018)]. Additional information will be provided in Section 2.2.4. By comparing the two types of data, one can theoretically isolate the influence of the LULC on the NSWS and subsequently, detect the changes over time.

2.2.3 Quality control of the near-surface wind speed observations

The analysis of the wind data was largely conducted using MATLAB R2021b. The entirety of the code for this study will not be discussed, but a few annotations are made here for a better understanding of the data analysis process: First, the location of all 59 stations is noted, including their longitude and latitude. The grid points of the ERA5 data set are then analysed and each wind station is matched with the closest corresponding grid point to its location. This step is conducted in order to enable the comparison of the observations and the reanalysis data. After merging, each data set is divided into three time periods. The starting period and the final period are set to five years to ensure that inter-annual variability within the data is mitigated. Their purpose is to detect NSWS changes before and after any potential changes that are being documented in the CLC maps. They will therefore give the best representation of the two components' linkage, provided such an entanglement exists. The information from all observational stations does not date back equally. This study chooses therefore to set equal starting points under the smallest common denominator for all 59 stations. The time periods are thus as follows:

1. 01.01.1996 00:00:00 AM – 31.12.2000 11:00:00 PM

2. 01.01.2001 00:00:00 AM – 31.12.2016 11:00:00 PM

3. 01.01.2017 00:00:00 AM – 31.12.2021 11:00:00 PM

To ensure appropriately high quality for the data, this study proceeds to index all observations that do not fulfill the quality standard set by SMHI as described in Section 2.2. The output of those observations is not considered and in the following suppressed. Following the dismissal, the data is visually checked for obvious gaps in order to identify potential distortion of the conveyed quality of information. In the final stage, all wind stations are once again checked for LULCC and SRC in their respective proximity, which was set to one kilometer as explained in the previous section. The examination is conducted on an individual level as well as on a holistic level. This step provides valuable information about the magnitude and the sign of the SRC at the stations individually and serves as a quantitative measure for the SRC strength around each station. It also provides information about the quality of the SRC in regards to representation of the country's SRC, i.e. it shows whether or not the data corresponds to the general trends in Sweden.

2.2.4 Comparison of observational data and reanalysis data

This project compares the above-mentioned observational SMHI NSWS data sets with the ERA5 data, in order to isolate the effect of LULCC and consequently SRC on the NSWS. To understand the intention behind this step, it is necessary to comprehend what the data entails. The Lagrangian form of the wind equation (Equation 1) describes the components that make up the wind vector and its velocity. It is applicable to the observational data, i.e. the real-time data, measured by the SMHI stations. The information in those data sets also contains the influence of the friction component as described in Section 2.2.1. Because the surroundings of the evaluated stations in this study, experience some form of LULCC, it is expected that the measured data will be influenced by changes of the drag force. The drag force decelerates the wind speed depending, among others, on the surface roughness as described in Section 1.2. Because we defined the wind as a function of the Lagrangian form of the wind equation and subsequently as a function of the surface roughness, one assumes that any changes thereof will alter the wind speed. As mentioned in Section 2.2.2, the ERA5 data does not include the changes of the land surface over time and is thus fixed. The observational data on the other hand is expected to be influenced by the varying LULC over time. We can assume that the differences between those two data sets can consequently be explained by the SRC. This method is not new. As a matter of fact, it has been used before by Kalnay & Kai (2003) to quantify the impact of Land use change (LUC) on surface warming, by Zhou et al. (2004) to look for the effect of LUC on the surface temperature in southeast China, by Li et al. (2008) to examine changes in the NSWS due to LUC in China and by Frauenfeld et al. (2005) to understand the temperature variability on the Tibetan Plateau. Wu et al. (2018) describe it as "Establishing a reference NSWS data set without LULCC effect" or also called the ODR method. ODR offers a favourable advantage over other methods. It is easily applicable, especially considering the location of many stations. Further information, on why the ODR-method is chosen, will be provided in Section 4. This study uses the ODR-method as shown in Equation 7:

$$f(z_0) = \frac{U_{\vec{Obs}}}{U_{\vec{ERA5}}} \tag{7}$$

Additionally to examining the holistic effect of SRC on the NSWS, this study will proceed to distinguish changes on the directional level. Each station's surrounding will be subdivided into four quadrants of 90 degrees (North-West, North-East, South-West and South-East) and the SRC will subsequently be documented. In the course of this process, the wind time series will also be divided into the respective directions. The ODR-method will thus be continued accordingly for the four cardinal directions, i.e. SRC will be compared to the respective upstream wind direction. This step serves as a measure to disentangle changes in NSWS and SR that do not align spatially and thus to clear up so-called noise. Noise can describe many factors, but in a more general sense, it describes internal and external factors that can obscure or distort the attributes and/or classification of the data [Hickey (1996)].

3 Results

This section will show the findings in relation to this study. It will follow the structure of the Methodology. That means, that the overall state of Europe's LULC in the year 2000 will be shown, followed up by the changes thereof, especially considering larger areas. Afterwards, the focus shifts towards Sweden and this study will provide the most important information about the alteration of the LULC for the study period. It will also point out which classes experienced the highest amount of change and their signs, i.e. did a certain category experience predominately gains or losses. All of these changes will be given in absolute and relative figures. Relative changes are measured as a change of the respective country's total land mass. In the course of this description, the resulting SRC in Sweden will also be shown. Finally, the focus will shift towards the analyzed wind stations and onto the LULCC in their proximity. This should give sufficient inside into the changes in Sweden before this section goes on to describe the results from the ODR-approach.

3.1 Land use and land cover in Europe in 2000

The European Continent showed vast differences across the latitudes as shown in Figure 1. A stark contrast existed between Southern/Central Europe and Northern Europe. The Scandinavian Countries (Norway, Sweden and Finland) as well as Iceland and northern Scotland (see the United Kingdom in Table 5) showed large amounts of vegetation as shown in Table 5. Despite their similarity in relative vegetation coverage, the type of vegetation differed between those countries. Finland, Sweden, as well as south-east Norway, were covered in large parts in coniferous forests ($\simeq$ 98.5 x 10^3 km^2, $\simeq$ 214.2 x 10^3 km^2 and $\simeq$ 59.0 x 10^3 km^2 respectively), although the northern parts of Sweden and Finland showed also larger amounts of Peat bogs ($\simeq$ 22.4 x 10^3 km^2 and $\simeq$ 28.8 x 10^3 km^2 respectively) and Grass-/Heathland ($\simeq$ 4.1 x 10^3 km^2 and $\simeq$ 28.9 x 10^3 km^2 respectively) due to the latitudinal and alpine characteristics of the territory. In contrast, western and northern Norway as well as Iceland were covered by Grass- and Heathland ($\simeq$ 45.8 x 10^3 km^2 and $\simeq$ 38.4 x 10^3 km^2 respectively), Peat bogs ($\simeq$ 21.1 x 10^3 km^2 and $\simeq$ 6.7 x 10^3 km^2 respectively) as well as Other LULC ($\simeq$ 50.6 x 10^3 km^2 and $\simeq$ 103.4 x 10^3 km^2 respectively). Iceland and Norway are highly influenced by an alpine topography and their relief did not allow for vegetation in many places. Thus, Other LULC corresponded most often to "Bare rocks" or "Glaciers and perpetual snow". In Norway, certain amounts of "Sparsely vegetated areas" could also be found. In Iceland, at the feet of the glaciers *Vatnajökull* and *Myrdalsjökull* large areas were covered by "Beaches - dunes - sands". A similar LULC was found in northern Scotland, where the landscape was dominated by Grass- and Heathland (48.1 x 10^3 km^2), Marshes and Peat bogs (5.3 x 10^3 km^2) and Other LULC (4.2 x 10^3 km^2). Contrary to Iceland and Norway, the Other LULC indicated almost exclusively "Sparsely vegetated areas" in the north of the United Kingdom.

The largest parts of western, central and eastern Europe were characterized by vast amounts of Agriculture, including the British Islands. The territorial coverage of Agriculture exceeded 30% in 31 out of 41 countries in this study, excluding Vatican City. For 25 out of 41 countries that limit exceeded 40%, reflecting the vast impact of Agriculture in Europe. The highest relative amount of Agriculture was found in Denmark (75.2%), San Marino (69.2%), Hungary (67.6%), Ireland (67.3%) and the Netherlands (67.3%). As expected, the relative amount of Agriculture in the northern Countries (Finland, Sweden, Norway and Iceland) was low at 8.7%, 8.7%, 4.9% and 2.3% respectively. In absolute terms, six countries exceeded 150 x 10^3 km^2 of agricultural and arable land: Turkey ($\simeq$ 332 x 10^3 km^2), France ($\simeq$ 328 x 10^3 km^2), Spain ($\simeq$ 230 x 10^3 km^2), Germany ($\simeq$ 214 x 10^3 km^2), Poland ($\simeq$ 197 x 10^3 km^2) and Italy ($\simeq$ 156 x 10^3 km^2). International and inter regional differences were common and apparent. In Ireland and the western United Kingdom Agriculture was most frequent in the form of Pastures, while in south-east England non-irrigated arable Land. Large areas of Pastures were also found in north-west and central France, the Netherlands and north-west Germany. Non-irrigated arable land was also most present in eastern Europe, such as Poland, Hungary, Romania and northern Serbia. Additionally, Denmark, northern Germany, north-east Italy and the regions around Paris and Toulouse in France were covered by large amounts of this LULC class. While some areas of non-irrigated arable land existed in southern Europe, large cultivation patterns of Vineyards as well as Olive- and Fruit trees were found in Portugal, Spain, southern France and southern Italy.

Table 1: Relative Land Use and Land Cover for each country and class in the year 2000 in %. The countries displayed correspond to how they exist today and not to the year 2000. Therefore this study distinguishes between Serbia, Kosovo and Montenegro. The classes displayed in this Table correspond to the reclassified classes shown in Table 8.

Country	Urban	Agriculture	Forest	Coniferous Forest	Grassland	Shrub	Peatbogs	Other LU	Water
Albania	1.7%	28.6%	23.4%	3.4%	10.8%	23.6%	0.1%	6.1%	2.3%
Andorra	0.0%	7.0%	2.0%	25.9%	23.2%	3.6%	0.0%	38.3%	0.0%
Austria	4.8%	32.3%	18.2%	26.3%	10.1%	0.1%	0.3%	7.1%	0.9%
Belgium	20.4%	57.5%	15.3%	4.5%	0.6%	0.5%	0.3%	0.1%	0.9%
Bosnia & Herzegovina	1.4%	36.7%	39.4%	4.7%	5.4%	10.3%	0.1%	1.4%	0.7%
Bulgaria	4.9%	51.5%	26.6%	4.8%	3.8%	6.7%	0.2%	0.5%	1.0%
Croatia	2.8%	40.8%	34.7%	1.8%	4.3%	12.3%	0.3%	1.1%	1.8%
Czechia	6.2%	57.3%	11.3%	21.7%	0.4%	2.3%	0.1%	0.0%	0.7%
Denmark	6.8%	75.8%	4.6%	4.2%	1.9%	1.9%	1.2%	0.1%	3.4%
Estonia	1.9%	32.2%	27.7%	17.9%	1.0%	8.8%	4.2%	0.1%	6.2%
Finland	1.3%	8.7%	28.3%	29.5%	1.2%	14.1%	6.7%	0.3%	9.8%
France	4.9%	59.9%	19.6%	6.5%	3.1%	3.3%	0.1%	1.6%	1.0%
Germany	8.1%	59.8%	13.3%	15.7%	0.7%	0.6%	0.4%	0.2%	1.3%
Greece	2.1%	39.8%	12.5%	5.5%	9.4%	26.5%	0.2%	1.8%	2.3%
Hungary	5.9%	67.6%	17.6%	1.1%	2.4%	2.6%	0.9%	0.0%	1.9%
Iceland	0.3%	2.3%	0.3%	0.0%	37.5%	0.2%	6.6%	49.5%	3.3%
Ireland	1.9%	67.3%	0.8%	3.4%	2.0%	5.2%	16.1%	0.6%	2.7%
Italy	4.7%	51.7%	22.4%	4.3%	5.5%	6.8%	0.1%	3.4%	1.3%
Kosovo	2.3%	40.6%	36.7%	2.1%	7.2%	9.2%	0.0%	1.6%	0.2%
Latvia	1.3%	43.9%	27.2%	14.5%	0.1%	8.4%	2.4%	0.1%	2.1%
Liechtenstein	13.9%	28.8%	26.9%	9.4%	15.1%	0.0%	0.0%	3.5%	2.4%
Lithuania	3.3%	61.3%	17.7%	11.3%	0.1%	3.4%	0.9%	0.0%	2.0%
Luxembourg	8.8%	55.1%	30.4%	4.5%	0.1%	1.0%	0.0%	0.0%	0.2%
Malta	27.5%	47.9%	0.4%	0.2%	0.0%	12.7%	0.0%	1.0%	10.2%
Monaco	46.9%	3.9%	8.5%	1.0%	7.0%	28.2%	0.0%	0.0%	4.4%
Montenegro	1.0%	16.4%	33.7%	7.2%	9.5%	23.7%	0.8%	5.7%	2.0%
Netherlands	12.1%	67.3%	4.1%	4.3%	2.0%	0.0%	1.0%	0.2%	8.8%
North Macedonia	1.5%	37.4%	32.0%	1.7%	7.4%	17.3%	0.1%	0.3%	2.2%
Norway	0.7%	4.9%	14.3%	18.5%	14.3%	1.7%	6.6%	32.4%	6.6%
Poland	4.0%	62.8%	12.2%	17.8%	0.1%	1.0%	0.3%	0.1%	1.6%
Portugal	3.2%	40.8%	25.4%	7.9%	5.6%	13.6%	0.1%	1.8%	1.6%
Romania	6.3%	56.9%	24.7%	4.7%	1.8%	2.5%	1.6%	0.2%	1.3%
San Marino	11.3%	69.2%	10.8%	0.0%	1.4%	7.3%	0.0%	0.0%	0.0%
Serbia	3.3%	56.9%	28.5%	1.1%	2.6%	5.8%	0.3%	0.3%	1.2%
Slovakia	5.5%	48.6%	30.0%	10.8%	0.8%	3.5%	0.1%	0.2%	0.6%
Slovenia	2.7%	34.3%	44.5%	12.1%	2.1%	2.2%	0.1%	1.4%	0.5%
Spain	1.6%	45.4%	15.3%	7.9%	7.0%	19.4%	0.1%	2.4%	0.9%
Sweden	1.3%	8.7%	8.0%	48.0%	6.5%	9.9%	6.5%	2.3%	8.8%
Switzerland	6.5%	28.5%	14.9%	15.4%	13.5%	0.4%	0.1%	17.3%	3.4%
Turkey	1.5%	42.6%	9.1%	6.1%	11.7%	10.8%	0.3%	16.0%	1.9%
United Kingdom	7.3%	58.3%	2.9%	5.2%	19.7%	0.8%	2.2%	1.7%	1.9%

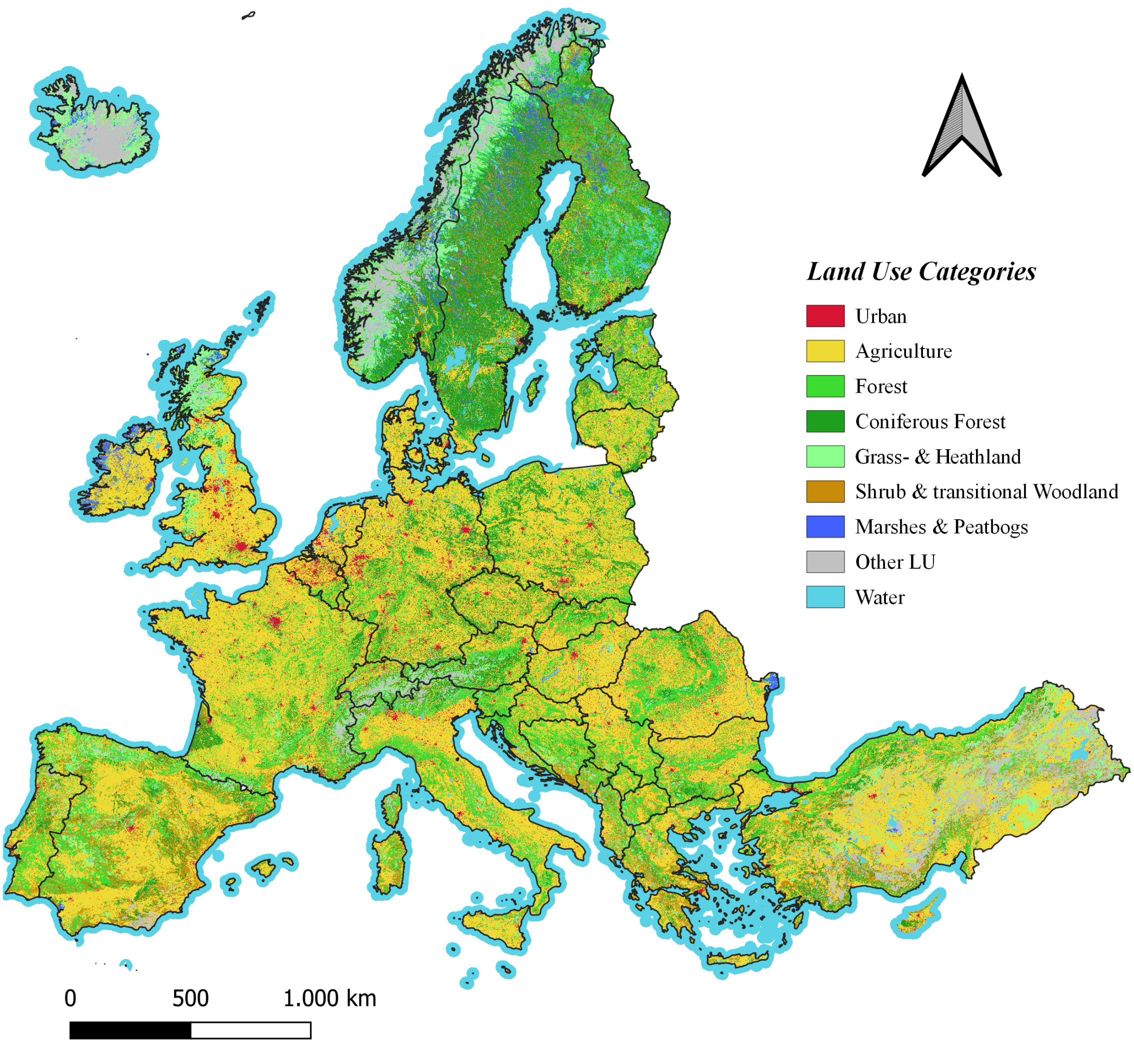

Figure 1: Land Use and Land Cover in Europe in 2000 at 100 meter resolution based on the CLC classification and reclassified according to Table 8.

Outside of the aforementioned forest areas in Finland, Sweden and southern Norway, few forests of sizeable dimensions existed across Europe. Due to the climate and extreme population densities all over the continent, shares of coniferous forests above 20% existed only in five out of 41 reviewed countries: Sweden (48.0%), Finland (29.5%), Austria (26.3%), Andorra (25.9%) and Czechia (21.7%). Higher numbers of mixed and deciduous forest were apparent in Europe. 15 out of 41 countries showed forest shares of more than 25%. They were exclusively located in eastern Europe, except for Portugal, Liechtenstein and Luxembourg. Most forest shares were found in the Balkan (Bosnia & Herzegovina, Bulgaria, Croatia, Kosovo, Montenegro, North Macedonia, Serbia and Slovenia), in the Baltics (Estonia and Latvia) as well as Slovakia. The ten countries where either deciduous/mixed forests or coniferous forests or both forest types combined exceeded 50 x 10^3 km^2 were: Finland, France, Germany, Italy, Norway, Poland, Romania, Spain, Sweden and Turkey. Forests were often found in the proximity to mountain ranges, such as the Alpes, the Appenines in Italy, the Black Forest in Germany, the Cantabrian Mountains in Spain, the Carpathian Mountains in the Balkan and the Dinaric Alps in the Balkan.

The extreme population density in Europe can also be recognized by the large amounts of urban areas throughout the continent. Especially the United Kingdom (7.3%), Germany (8.1%) and the so called BENELUX-states (Belgium (20.4%), the Netherlands (12.1%) and Luxembourg (8.8%)) show high numbers of urbanization. Comparatively lower Urban densities were found in the Balkan and in Northern Europe, including the Baltic Countries and Scandinavia. The common share of Urban areas was approximately 1-2%. The largest total Urban areas were naturally found in the countries with the highest populations, i.e. Germany, France and the United Kingdom. Contrary to the obvious trend, Romania had the fourth highest amount of urban areas, before Italy, Poland and Turkey. Finally, comparatively low extents were found in Spain.

Ultimately, the LULC conditions were found to be noticeably complex. Most regions were subjected to a number of different LULC classes. Generally, the LULC correlated with the topography and the prevailing climate conditions, e.g. coniferous forests were most often found in boreal and alpine regions, whereas agriculture was found most prominently in plains.

3.2 Land use and land cover changes in Europe [2000-2018]

Precisely as the LULC, the same patterns of complexity were found for the LULCC in all countries. The changes were usually minor in terms of area, i.e. in the order of a few hectares and occasionally went up in size to a few square kilometre. Additionally, the changes were most often spatially scattered. Thus, only few locations with extensive LULCC were found across the continent, where the changes were of the same sign as well as the same classification. This reasoning is inferred by the spatial and numerical information from Figure 2 and 9, as well as Table 2 showing the respective changes as a relative number of the total landmass that each country governs and Table 6 showing the effective LULCC for each country and class in km^2.

An increase of urban areas (Urbanization) across the continent was one trend found to be true in every country but Andorra, Bulgaria, Finland and Romania: In Romania and Bulgaria the Urbanization regressed, while it stagnated in Andorra and Finland. The other 37 countries showed some form of positive numerical trend in that regard, with Kosovo, Liechtenstein, the Netherlands, Poland and San Marino showing increases of at least 2%. Urbanization was relatively often found in the areas of already existing metropolitan areas, such as Madrid, Paris, London, Warsaw, Bucharest, Tirane and Istanbul. Many more of these examples exist. While positive, the development of urban areas in the Nordic countries was rather small at circa 0.016 x 10^3 km^2, circa 0.59 x 10^3 km^2, circa 0.27 x 10^3 km^2 and circa 0.06 x 10^3 km^2 for Finland, Sweden, Norway and Iceland respectively. The largest absolute increases were found in Europe's most populous countries: Poland ($\simeq$ 6.87 x 10^3 km^2), France ($\simeq$ 5.48 x 10^3 km^2), Germany ($\simeq$ 4.66 x 10^3 km^2), and Spain ($\simeq$ 4.55 x 10^3 km^2).

Table 2: Relative Land Use and Land Cover Change for each country and class in % corresponding to each country's total land mass. Negative numbers equate to a decrease in the respective class and country. At the same time, a positive number describes an increase. The classes displayed in this Table correspond to the reclassified classes shown in Table 8.

Country	Urban	Agriculture	Forest	Coniferous Forest	Grassland	Shrub	Peatbogs	Other	Water
Albania	1.0%	-0.4%	-1.6%	-0.5%	0.6%	0.2%	0.0%	0.6%	0.2%
Andorra	0.0%	-0.5%	0.3%	0.3%	2.5%	-1.9%	0.0%	-0.7%	0.1%
Austria	1.1%	-0.5%	-0.2%	-0.7%	-0.3%	0.5%	0.0%	0.0%	0.0%
Belgium	0.5%	-0.5%	0.1%	-0.1%	0.0%	0.1%	0.0%	0.0%	0.0%
Bosnia & Herzegovina	0.4%	-3.6%	1.9%	0.1%	0.8%	-0.3%	0.0%	0.8%	0.0%
Bulgaria	-0.1%	0.1%	-0.1%	-0.1%	0.1%	0.2%	0.0%	0.0%	0.1%
Croatia	0.8%	-0.6%	-0.8%	-0.1%	0.0%	0.7%	0.0%	0.0%	0.0%
Czechia	0.4%	-0.5%	0.4%	-0.4%	0.0%	0.1%	0.0%	0.0%	0.0%
Denmark	1.0%	-2.3%	0.4%	-0.3%	0.0%	1.1%	0.0%	0.0%	0.1%
Estonia	0.2%	-0.9%	0.9%	-0.4%	-0.2%	0.0%	0.3%	0.0%	0.0%
Finland	0.0%	-0.4%	2.2%	3.3%	0.8%	-5.9%	-0.3%	0.2%	0.1%
France	1.0%	-0.9%	0.4%	-0.3%	-0.0%	-0.2%	0.0%	0.0%	0.1%
Germany	1.3%	-2.5%	0.8%	0.4%	0.1%	0.1%	-0.1%	-0.1%	0.1%
Greece	1.0%	-1.2%	1.8%	0.2%	-1.5%	-1.2%	0.0%	0.8%	0.2%
Hungary	0.6%	-2.7%	0.2%	-0.1%	0.0%	1.9%	0.0%	0.0%	0.0%
Iceland	0.1%	0.1%	0.2%	0.0%	-0.5%	0.1%	-0.1%	0.1%	0.0%
Ireland	0.4%	0.4%	0.9%	1.5%	-0.1%	-2.1%	-1.5%	0.7%	-0.1%
Italy	0.7%	-0.4%	0.2%	0.0%	-2.3%	-0.3%	0.0%	2.0%	0.0%
Kosovo	2.4%	-2.5%	0.4%	0.0%	-0.1%	-0.5%	0.0%	0.3%	0.0%
Latvia	0.7%	-4.2%	-2.3%	-2.0%	0.1%	7.4%	0.1%	0.0%	0.2%
Liechtenstein	2.1%	-5.3%	1.4%	4.7%	-2.7%	0.3%	0.6%	-0.9%	-0.2%
Lithuania	0.1%	-2.6%	1.1%	0.0%	0.0%	1.4%	0.0%	0.0%	0.1%
Luxembourg	1.8%	-2.2%	1.1%	0.1%	-0.1%	-0.7%	0.0%	0.0%	0.0%
Malta	0.3%	0.2%	0.0%	0.0%	0.0%	-0.3%	0.0%	0.0%	-0.1%
Monaco	0.5%	-0.1%	-0.3%	1.9%	-0.1%	-2.1%	0.0%	0.0%	0.1%
Montenegro	0.8%	-0.5%	0.3%	-0.1%	-2.1%	-1.7%	0.0%	3.1%	0.0%
Netherlands	2.4%	-3.4%	0.1%	-0.1%	0.6%	0.1%	0.3%	0.0%	0.1%
North Macedonia	0.3%	-1.5%	-1.8%	-0.1%	1.1%	1.3%	0.0%	0.5%	0.1%
Norway	0.1%	0.0%	0.0%	-0.5%	0.0%	0.4%	0.0%	0.0%	0.0%
Poland	2.2%	-4.1%	0.8%	0.2%	0.0%	0.9%	0.0%	0.0%	0.1%
Portugal	0.7%	-1.4%	-3.5%	-2.9%	0.6%	6.6%	0.0%	-0.4%	0.3%
Romania	-0.7%	0.2%	0.7%	-0.1%	1.0%	-0.6%	-0.4%	-0.1%	0.0%
San Marino	2.9%	-2.2%	-0.9%	0.0%	-0.6%	0.8%	0.0%	0.0%	0.0%
Serbia	0.5%	-2.1%	0.3%	0.1%	-0.1%	1.2%	0.1%	0.0%	0.0%
Slovakia	0.7%	-1.3%	1.7%	-0.7%	0.0%	-0.4%	0.0%	0.0%	0.0%
Slovenia	0.8%	-0.6%	0.0%	-0.2%	-0.2%	0.2%	0.0%	0.0%	0.0%
Spain	0.9%	-2.1%	1.7%	1.4%	3.6%	-5.2%	0.0%	-0.3%	0.1%
Sweden	0.1%	0.1%	1.5%	1.2%	0.0%	-3.1%	0.3%	0.1%	-0.1%
Switzerland	0.4%	-1.0%	-0.4%	-1.2%	-0.2%	2.7%	0.0%	-0.3%	0.0%
Turkey	0.4%	1.1%	-0.6%	0.2%	-0.1%	0.5%	0.0%	-1.6%	0.2%
United Kingdom	1.3%	-2.6%	0.4%	-0.2%	-0.1%	0.8%	0.8%	-0.6%	0.1%

An opposing trend of LULCC was found for the Agriculture class. Despite its major role in 2000, the amount of cultivated land has decreased across Europe. While seven countries displayed a positive areal trend, with Bulgaria (0.1%), Iceland (0.1%), Ireland (0.4%), Malta (0.2%), Romania (0.2%), Sweden (0.1%) and Turkey (1.1%), the rest of Europe's agricultural land diminished. This decrease regularly exceeded 2%, i.e. in 15 out of 41 countries; among those also larger countries in size and population such as Poland, Spain and the United Kingdom. The agricultural changes were relatively uniformly distributed in all countries, except for Romania and the United Kingdom. In Romania two larger areas were found in the centre of the country, where farmland was removed. In the United Kingdom, losses occurred mainly in central England, as well as southern Scotland and in north-west Wales. At the same time, it gained some farmland in central Wales.

The same levels of consistency in sign and magnitude as the Agriculture changes could not be found for Af- and Reforestation in Europe. Forestation efforts were generally low, which can be seen in the number of countries with forest and/or coniferous forest increases of at least 1% were limited to eleven. In Slovakia, this trend was even further reduced. While a 1.7% increase in forest area occurred, 0.7% of coniferous forest area was lost. The largest absolute increases of forest and coniferous forest cover were found in Finland ($\simeq$ 7.4 x 10^3 and $\simeq$ 11 x 10^3 km^2), Spain ($\simeq$ 8.5 x 10^3 and $\simeq$ 6.9 x 10^3 km^2), Sweden ($\simeq$ 6.6 x 10^3 and $\simeq$ 5.5 x 10^3 km^2), Germany ($\simeq$ 3 x 10^3 and $\simeq$ 1.2 x 10^3 km^2) and in Poland ($\simeq$ 2.5 x 10^3 and $\simeq$ 0.7 x 10^3 km^2). Contrarily, the largest effective decreases were found in Portugal ($\simeq$ -3.2 x 10^3 and $\simeq$ -2.6 x 10^3 km^2), Turkey ($\simeq$ -5 x 10^3 and $\simeq$ +1.5 x 10^3 km^2), Latvia ($\simeq$ -1.5 x 10^3 and $\simeq$ -1.3 x 10^3 km^2) and in Norway ($\simeq$ +0.05 x 10^3 and $\simeq$ -1.5 x 10^3 km^2). The sum of all forest and coniferous forest related changes in Table 6 result in a gain of circa 47 x 10^3 km^2 forest cover. Approximately 29.3 x 10^3 km^2 are a result of forest increases, while circa 17.7 x 10^3 km^2 of coniferous forest cover was gained.

Another indicator of forestation and deforestation is the development of transitional Woodland and shrub, as described in Section 2.1. These changes were diverse over the considered time period. Most countries showed either some form of increase or decrease, but it rarely exceeded 1.5% of the countries total land mass. A few exceptions were present, with four countries having an increase of more than 1.5% and seven countries with decrease of at least 1.5% (see Table 2). Finland (-5.94%, $\simeq$ -19.9 x 10^3 km^2), Sweden (-3.15%, $\simeq$ -14 x 10^3 km^2) and Spain (-5.15%, $\simeq$ -26.1 x 10^3 km^2) saw vast decreases. The changes of this specific class should be taken with caution in the case of Spain, because of the explanation given in Section 2.1. Shrub & transitional Woodland increased in Latvia by 7,42% of its total landmass (4.8 x 10^3 km^2) and by 6,61% in Portugal (6 x 10^3 km^2), indicating an opposite picture.

Overall, the largest effective LULC decreases in Europe were found to be Agricultural Land (approximately -56.6 x 10^3 km^2) as well as Shrub & transitional Woodland (approximately -39.6 x 10^3 km^2), as shown in Figure 3. As a reference point, the size of Croatia is circa 56.6 x 10^3 km^2 and the size of Switzerland is circa 41.3 x 10^3 km^2. Most frequently, the decrease of Agricultural Land was due to conversions towards Urban areas (47.1 x 10^3 km^2), Forests (35.9 x 10^3 km^2) and Grass- & Heathland (26.6 x 10^3 km^2). Increases of the Agricultural land class were most prominently a result of conversion from Grass- & Heathland (27.9 x 10^3 km^2), Shrub % transitional Woodland (24.2 x 10^3 km^2) as well as Forests (23.7 x 10^3 km^2). Shrub & transitional Woodland was most often converted or naturally transitioned into Coniferous Forests (72.1 x 10^3 km^2), Forests (63.1 x 10^3 km^2) and Agricultural Land (24.2 x 10^3 km^2), as mentioned above. The largest net increases in Europe were found for Urban areas (approximately 38 x 10^3 km^2) as well as Forests (approximately 29.4 x 10^3 km^2), which include Agroforestry areas, Broad-leaved forests and Mixed forests. The main contributor to the Urbanization was a decrease in Agricultural Land (47.1 x 10^3 km^2). Oppositely, the main decrease of Urban areas was the conversion to Agricultural Land (13.9 x 10^3 km^2). Forestation took mostly place in a few countries, as described above and shown in Table 6. These conversions had two noticeable sources: Shrub & transitional Woodland (63.1 x 10^3 km^2) as well as Agricultural Land (35.9 x 10^3 km^2). The same classes were also the most prominent factors in conversion of Forests. 41.5 x 10^3 km^2 of Forest were converted or transitioned into Shrub & transitional Woodland and 23.7 x 10^3 km^2 were converted into Agricultural Land. Few changes were found for Marshes & Peatbogs, because the transition of Marshes & Peatbogs $\leftrightarrow$ Grassland & Heathland was disregarded. The justification for this step is described in Section 2.1.

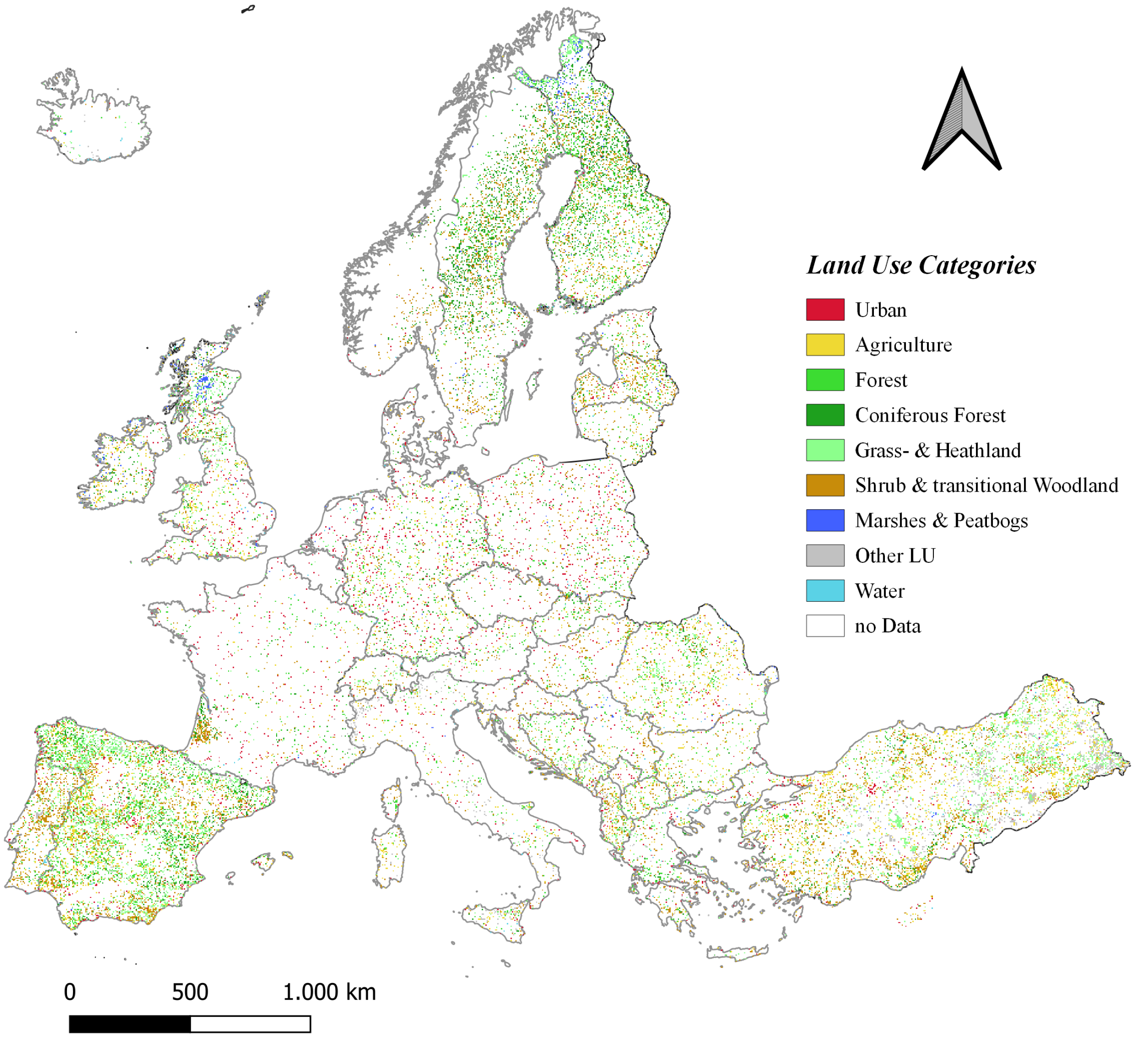

Figure 2: Land Use and Land Cover Changes in Europe between 2000 and 2018. The changes displayed correspond to the LULC that could be found after the alteration. The resolution is set to five km.

The LULCC in Europe did not happen simultaneously. Some time frames showed larger numbers of alterations in certain countries or regions than others. Prime examples are the Iberian Peninsula as well as Scandinavia, predominantly Finland and Sweden. The time period of 2000-2006 showed vast amounts of change all over the Iberian Peninsula. Despite its scattered nature, changes often resulted in increases of Grass- & Heathland in Spain, which one can see numerically in said class in Table 6 and 2. Changes in Portugal included large increases of Shrub & Heathland. The subsequent time periods of 2006-2012 and 2012-2018 saw comparatively little change in the region. At the same time a reversed picture was observable in Finland and Sweden. Both, Finland

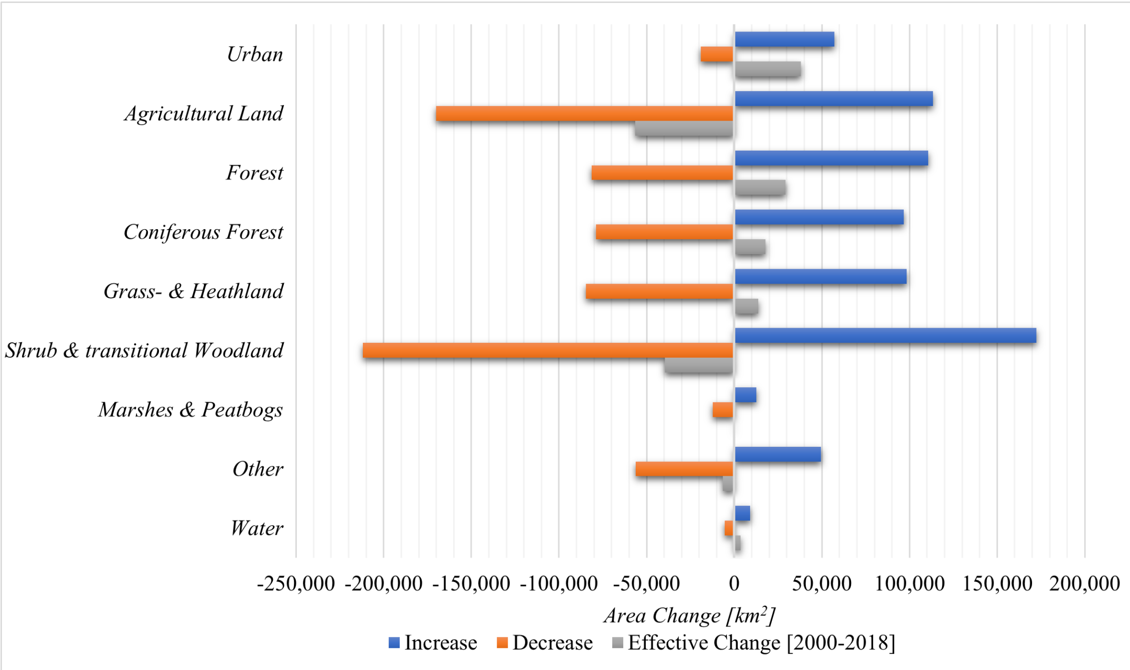

Figure 3: Land Use and Land Cover Change in Europe by class. Each class includes three bars: Blue shows the total summed increase of the respective class across all countries; orange shows the total summed decrease of the respective class across all countries; grey shows the total effective LULCC (Increase minus Decrease) of the respective class across all countries. The classes displayed in this Figure correspond to the reclassification shown in Table 8.

and Sweden saw a visibly smaller number of changes in the first period (2000-2006) than in the second period (2006-2012). While the changes in these two countries were consistently inconsistent, meaning scattered, moderate in size and not of the same size, only slight trends were observable. Both countries showed weak signs of deforestation in the first time frame and a subsequent increase of Shrub & transitional Woodland. In the second time frame that sign reversed and strong signs of forestation were found, including increments for both forest classes. It is noteworthy, that although a overall trend of forestation occurred, most often these changes were accompanied by some form of deforestation on the local scale. Uniform change was rarely found in this study. The above mentioned changes in the second period persisted for the third period (2012-2018) for both Finland and Sweden, although with reduced strength and density. In the United Kingdom, LULCC were comparatively intense during the first time frame, with most of the above mentioned changes occurring then. Most apparent were the losses of cultivated land in southern Scotland and northern England as well as the gain of said class in central Wales. Additionally, gains of Marshes & Peatbogs and geographical shifts of Grass- & Heathland were found in central and northern Scotland. In the following two periods, little change occurred across the country, except for slight deforestation acts north of the Scottish-English border. Most of Poland's Urbanization efforts happened in the first time stretch, where many of those areas were borrowed from farmland, which explains partly its massive 4.1% decrease in cultivated land. These changes continued into the second interval, although with less intensity. Just like in Poland, but with less intensity, Urbanization efforts and reduction of farmland took place in Germany. These changes occurred almost exclusively in between 2006 and 2012 and explain its Urbanization of 1.3% and its 2.5% decrease of Agricultural Land.

One trend that was found throughout Europe was the absence of LULCC during the third time frame. While large areas were converted or classes shifted within a region in the first two time frames, these changes did not continue in this last interval. The only two countries with nation wide changes were as already mentioned Finland and Sweden. A few other regions with alterations were found in Portugal and in France, south of Bordeaux. Further changes were negligibly small.

3.3 Alterations in Sweden

This section puts a focus on the LULCC in Sweden, i.e. dives also into the chronological differences. Subsequently, the resulting/emerging SRC will be introduced, with a focus on the regional differences. The information given in this section refers to Table 3 and Table 4. Precisely as in the previous Section, the author emphasizes the hazy distinction between the classes Forest and Coniferous forest.

3.3.1 Land use and land cover changes

The bigger picture was already given in the previous section; the overall trend in Sweden has been forestation between 2000 and 2018. Concerning overall forestation, an inherent North-South trend was found. The largest amounts of these forestation efforts took place in the Swedish region of *Norrland*. Especially, the counties Norrbotten and Jämtland showed both major signs of forestation, each with circa 3.3 x 10^3 km^2 of total forestation in the respective Iäns. The notable difference is the amount of specifically Coniferous forests, that were found. While the Coniferous forest class made up approximately 75% of all newly grown forests in Norrland, this number decreased to circa 40% in Jämtland. Norrland is the most northern Iän in Sweden and the climate corresponds to that. Effective deforestation was largely absent in Norrland, with the sole exception of the Coniferous forests in Västernorrland (-0.074 x 10^3 km^2). This Iän experienced at the same time an increase of approximately 1.35 x 10^3 km^2 within the Forest class. The total forestation gain in Norrland sums up to $\simeq$ 10.4 x 10^3 km^2. In Svealand, the central region of Sweden, most Iäns were found to have had even amounts of forestation and deforestation, except for Dalarna with circa 0.2 x 10^3 and 1.7 x 10^3 km^2 of Forest class and Coniferous class increase, respectively. Further south in Götaland, changes seemed to be of stronger magnitude than in Svealand. In total, the changes were approximately even, although a slight west-east gradient was apparent. In the western Iäns Halland, Jönköping, Kronoberg, Skåne and Västra Götaland the total sign of change was negative, i.e. deforestation took place. These changes were not reproduced in the eastern Iäns Blekinge, Gotland, Kalmar and Östergötland. Whenever deforestation occurred in Sweden over said period, those seemed to be induced by the negative trend of Coniferous forest class and not the Forest class.

Table 3: LULCC in Sweden, subdivided into the 21 national counties (Iän). The region of each county is indicated by the bracketed notes behind each Iän: (N) = Norrland, (S) = Svealand and (G) = Götaland . Negative numbers equate to a decrease in the respective class and county. At the same time, a positive number describes an increase. The classes displayed in this Table correspond to the reclassified classes shown in Table 8.

Iän	Urban	Agriculture	Forest	Coniferous Forest	Grassland	Shrub	Peatbogs	Other	Water
Norrbotten (N)	46.7	13.2	856.5	2468.1	3.1	-3398.9	113.8	10.5	-113.2
Jämtland (N)	33.2	18.1	1952.2	1364.2	-47.9	-3473.3	248.3	35.2	-130.1
Västerbotten (N)	26.9	29.2	716.2	1262.4	124.6	-2309.4	218.8	-0.7	-68.0
Västernorrland (N)	15.0	59.7	1350.2	-74.1	0.0	-1476.2	148.4	19.6	-42.7
Gävleborg (N)	23.2	34.3	410.6	74.8	-0.8	-569.1	77.5	0.0	-50.5
Dalarna (S)	52.1	-15.4	208.6	1721.9	7.0	-1993.9	107.9	-4.3	-84.0
Örebro (S)	24.3	12.8	112.3	114.1	0.0	-272.4	24.2	0.9	-16.1
Södermanland (S)	12.5	26.3	13.2	-60.4	0.0	9.4	3.5	0.0	-4.5
Stockholm (S)	101.3	-30.3	38.6	-14.3	0.0	-97.9	1.3	5.0	-3.6
Uppsala (S)	38.3	-4.5	190.5	-114.5	0.0	-122.2	24.4	0.0	-12.1
Värmland (S)	12.1	37.7	113.4	339.1	0.0	-511.4	44.2	-0.4	-34.7
Västmanland (S)	12.1	7.0	69.6	-72.4	0.0	-147.7	16.0	119.6	-4.2
Blekinge (G)	6.7	7.6	42.0	-39.2	0.0	-15.0	1.2	0.2	-3.5
Gotland (G)	12.7	-3.0	1.8	5.1	0.0	-46.0	3.3	29.4	-3.4
Halland (G)	1.3	23.3	10.2	-219.0	-1.3	173.2	12.9	0.2	-0.6
Jönköping (G)	13.8	15.3	65.0	-121.5	0.0	-19.2	50.3	0.0	-3.8
Kalmar (G)	21.7	16.5	220.0	137.5	0.2	-395.2	11.3	-0.3	-11.9
Kronoberg (G)	16.3	41.1	40.1	-666.9	0.0	506.6	82.9	0.0	-20.3
Östergötland (G)	16.3	-1.4	75.6	21.7	1.3	-106.8	8.0	0.0	-14.6
Skåne (G)	48.2	-23.0	100.4	-126.2	-0.3	-24.7	30.6	0.3	-5.3
Västra Götaland (G)	56.7	45.3	81.5	-483.1	0.0	206.1	82.1	9.3	2.2

A similar trend of opposite sign was found for the Shrub & transitional Woodland class. The effective decrease of Shrub in Norrland was found to be enormous, ranging from roughly -0.57 x 10^3 km^2 in Gäveleborgs Iän to as much as circa -3.5 x 10^3 km^2 in Jämtland. The total decrease in Norrland sums up to approximately 11.2 x 10^3 km^2. Changes in Svealand and Götaland are more diverse than in Norrland, with significantly lower dimensions. Additionally, a few Iäns showed a slight to strong increase of Shrub & transitional Woodland: Södermanland ($\simeq$ 0.009 x 10^3 km^2), Halland ($\simeq$ 0.17 x 10^3 km^2), Kronoberg ($\simeq$ 0.5 x 10^3 km^2) and Västra Götaland ($\simeq$ 0.2 x 10^3 km^2). Opposing trends for forestation and Shrub & transitional Woodland were found all over Sweden. It means, that when forestation efforts persisted, they usually came along with decreases in Shrub & transitional Woodland surface area and vice versa. This trend matched up well in sign and magnitude in all counties, differing rarely beyond a few tens of square kilometre. The only exception was found to be Västmanlands Iän, where the total forest area decreased slightly and additionally the surface area of Shrub & transitional Woodland decreased. A clear increase of the Other LULC category was found. A closer inspection showed that the increase was due to a large forest fire between 2012 and 2018, that resulted in a transition of Coniferous forest to Burned Area north of Västerås. Comparatively small, but positive, Urban area changes were found throughout the whole country. Most notably, Urbanization took place in Stockholms Iän ($\simeq$ 0.1 x 10^3 km^2) and Västra Götalands Iän ($\simeq$ 0.06 x 10^3 km^2), which include among others the two biggest Swedish cities Stockholm and Gothenburg. Agricultural changes too were found to be comparatively insignificant as well as inconsistent. No Iän showed changes of more than 0.06 x 10^3 km^2, with that exact maximum found in Västernorrland. Almost no change was found for Grass- & Heathland. The only notable exceptions are Jämtland where a slight decrease occurred ($\simeq$ 0.05 x 10^3 km^2) and Västerbotten where a slight increase was found ($\simeq$ 0.12 x 10^3 km^2). Finally, medium positive signs for Marshes & Peatbogs were located in Norrland, with up to 0.25 x 10^3 km^2 in Jämtland. Outside of Norrland, alterations were rather low with the only change worth noting in Dalarna ($\simeq$ 0.1 x 10^3 km^2). As noted earlier, LULCC occurred at different points in time. Generally, the largest number of changes happened between 2006 and 2011. These changes were largely a product of forestation efforts and some degree of Shrub & transitional Woodland reduction. Just as the raw numbers indicate, most changes and the highest density of changes occurred in Norrland, especially east of the mountainous regions. The further south in Sweden one looks (Svealand and Götaland), the more the LULCC density decreases. The periods 2006-2011 and 2012-2018 have largely common signs of change, despite differing in magnitude, with the largest number of changes arising as forestation. Contrarily, 2000-2005 indicated the opposite sign, with larger numbers of deforestation and consequently an increase of Shrub & transitional Woodland. These changes were quite observable in Norrland, but less frequent in Svealand and Götaland with the exception of Kronobergs Iän in the south of Sweden. As a result, Kronoberg experienced a strong sign of deforestation (Coniferous forest).

3.3.2 Surface roughness changes

By and large, looking at the mean SRC in Sweden, the alterations are minimal with 0.001 m over the entire time frame (2000-2018). Given the assumption of a more regional impact, it is worth looking into the changes on a smaller spatial and temporal scale, in order to understand if the impact may differ from the national mean. The mean SRC seemed to differ a lot over time in Sweden, just as previously mentioned for the sign of (de-)forestation. During the first time frame (2000-2005), the sign and magnitude of the SRC were consistent across all three regions. In absolute terms, Svealand and Götaland showed naturally less SRC than Norrland. Relative to the size of the respective regions, all three showed similar amounts of altered areas. Just as described in the previous section, the first time frame encountered the least area change, at approximately 2.7% on mean. At the same time, this period showed also the most consistent SRC. It varied between -0.002 and -0.003 meter on the regional level and averaged to -0.002 meter on the national level. The second time frame (2006-2011) induced the most alterations of the total land mass, ranging from 5.7% in Götaland to 10.1% and 10.6% in Svealand and Norrland, respectively. Contrarily to the first time frame, the mean SRC was less consistent. Svealand and Norrland encountered a small rise of SR, it sank however marginally in Götaland. The actual changes were scattered vigorously across the country and the sign differed on small scales. However, on a larger scale, a east-west trend was evident, with the western Iäns encountering more negative SRC than positive and a clear increase in SR in Kalmars Iän, Östergotlands Iän and in parts in Blekinge. The last period 2012-2018 saw marginal increases of the mean SR in Norrland and Svealand, with 0.001 and 0.002 meter in Norrland and Svealand, respectively. Götaland too showed an increase, although lower in strength (0.0001 m). Additionally, the amount of area change was relatively low, compared to the previous time span. Two percent of Götaland's surface area encountered some form of roughness length change; Svealand and Norrland saw five and four percent, respectively. The changes in and of themselves were found to be sizeable. The total alteration combined for 68.1 x 10^3 km^2, which reflects roughly 15% of Sweden's entire land mass. Ultimately, these changes offset each other partially on this scale and over time. It needs to be noted that all of these changes were scaled across the entire respective region and not only the areas that were affected by some form of SRC.

Finally, as mentioned in Section 2.2.3, to check the quality of the SRC for the ODR-method, this study documents the number of alterations and calculates the mean SRC across the one kilometer radii of all stations. This review showed that the areas surrounding the stations matched up considerably well in terms of altered area, but deviated from the mean SRC in Sweden. More precisely, the surroundings encounter some form of SRC at a rate of 3.76% in 2000-2005, 10.27% in 2006-2011 and 3.62% in 2012-2018. This is measured as a mean of the total amount of area encompassing the stations; the amount and mean SRC varied on an individual level. This matches up well with the previously demonstrated area changes in Sweden. The mean SRC compares well with the national mean. In 2000-2005, the SRC of station area showed a mean of -0.003 meter for the stations and -0.002 for Sweden. That trend continues in the ensuing time frames, shown by the parity of the stations SRC with 0.006 in 2006-2011 and 0.001 in 2012-2018 compared to the mean SRC in Sweden of 0.004 in 2006-2011 and 0.001 in 2012-2018.

Table 4: Surface Roughness Changes in Sweden, subdivided into four Regions. Each region consists of a number of counties (Iän). The counties for each Region are as follows: 1. Norrland (Gävleborgs Iän, Jämtlands Iän, Norrbottens Iän, Västerbottens Iän & Västernorrlands Iän), 2. Svealand (Dalarnas Iän, Örebro Iän, Södermalms Iän, Stockholms Iän, Uppsala Iän, Värmlands Iän & Västmanlands Iän) and 3. Götaland (Blekinge Iän, Gotlands Iän, Hallands Iän, Jönköpings Iän, Kalmar Iän, Kronobergs Iän, Östergötlands Iän, Skåne Iän & Västra Götalands Iän). The Mean SRC [m] shows the average change over the entire area of the respective region. The column Area [km^2] shows the total amount of surface area, that has undergone some form of SRC.

Sweden			
Time Period	Mean SRC [m]	Area [km2]	Relative Area Change
2000-2005	-0.002	12135.6	2.7%
2006-2011	0.004	39802.4	8.9%
2012-2018	0.001	16165.1	3.6%
2000-2018	0.001	68103.2	15.2%

Norrland			
Time Period	Mean SRC [m]	Area [km2]	Relative Area Change
2000-2005	-0.003	7604.6	2.9%
2006-2011	0.006	26408.7	10.1%
2012-2018	0.001	10322.5	4.0%
2000-2018	0.0015	44335.8	17.0%

Svealand			
Time Period	Mean SRC [m]	Area [km2]	Relative Area Change
2000-2005	-0.002	2235.95	2.8%
2006-2011	0.005	8595.2	10.6%
2012-2018	0.002	4018.7	5.0%
2000-2018	0.0014	14849.8	18.4%

Götaland			
Time Period	Mean SRC [m]	Area [km2]	Relative Area Change
2000-2005	-0.003	2345.6	2.7%
2006-2011	-0.001	4988.4	5.7%
2012-2018	0.0001	1870.4	2.1%
2000-2018	-0.001	9204.4	10.5%

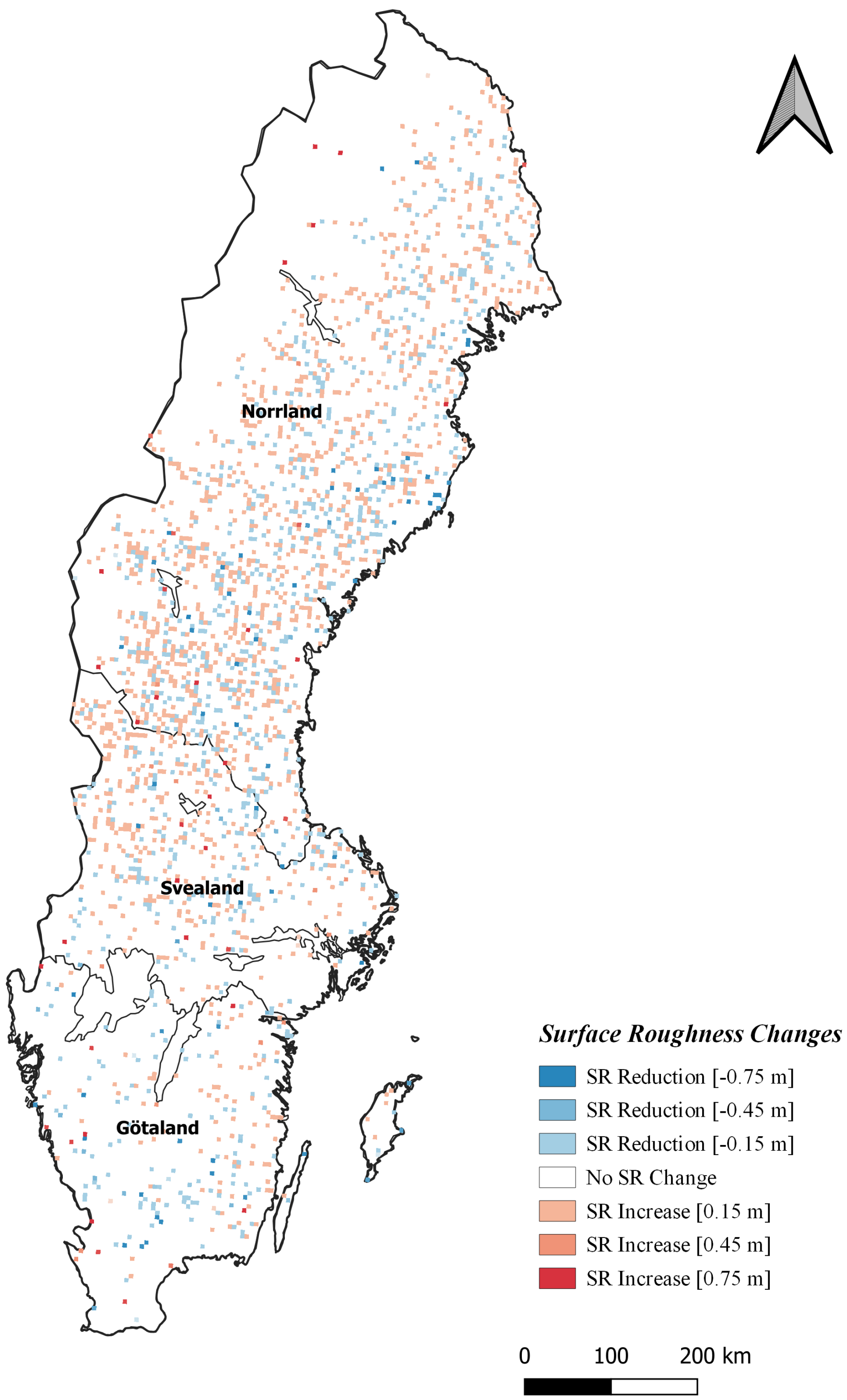

Figure 4: Surface Roughness Changes in Sweden between 2000 and 2018 at five km resolution.

3.4 The impact on near-surface wind speed

The quality control of all wind data sets showed that before the year 2006, in some cases even later, most stations measured the wind direction and velocity every three hours. Although the stations most often produced output in between the three hourly intervals, these values were usually flagged as low-quality or *yellow* as defined by SMHI. The flagged data points were thus removed, to ensure that the utilized data was of high quality, leaving on average one-third of the original data in those time frames. In later years (2007-2021), measurements were increased to an hourly interval and the quality indicator showed no reason for concern. This fact leads to a considerably smaller number of data points in periods one compared to period three. Extremely few values were flagged as low quality for the latter periods throughout all 59 stations. Lastly, the wind speed distribution for all stations was checked and is shown in Figure 5. Measurements within 0-3 m s^{-1} sum up to $\simeq$ 66% of the total available data, which is considerable and should be noted.

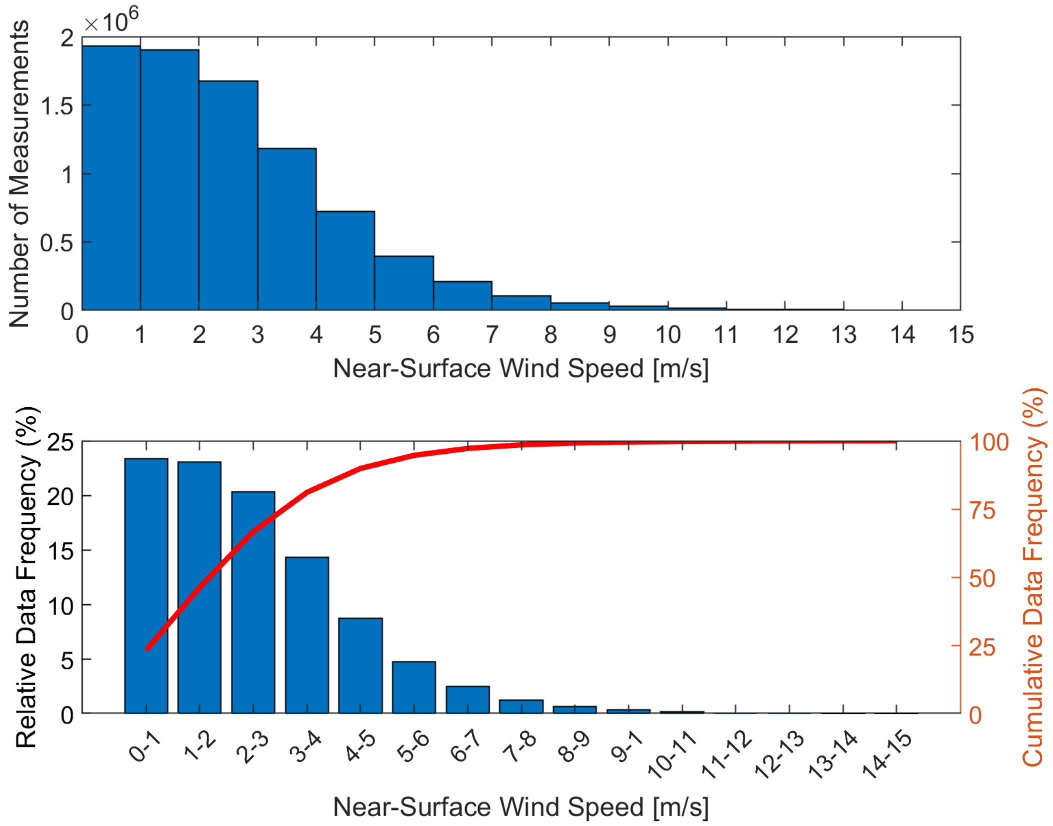

Figure 5: The cumulative NSWS distribution and relative distribution of all 59 wind stations. The first subplot shows the wind speed of all recorded data points across all stations. The second subplot corresponds to the first subplot and shows the relative distribution of the respective wind speed measurements.

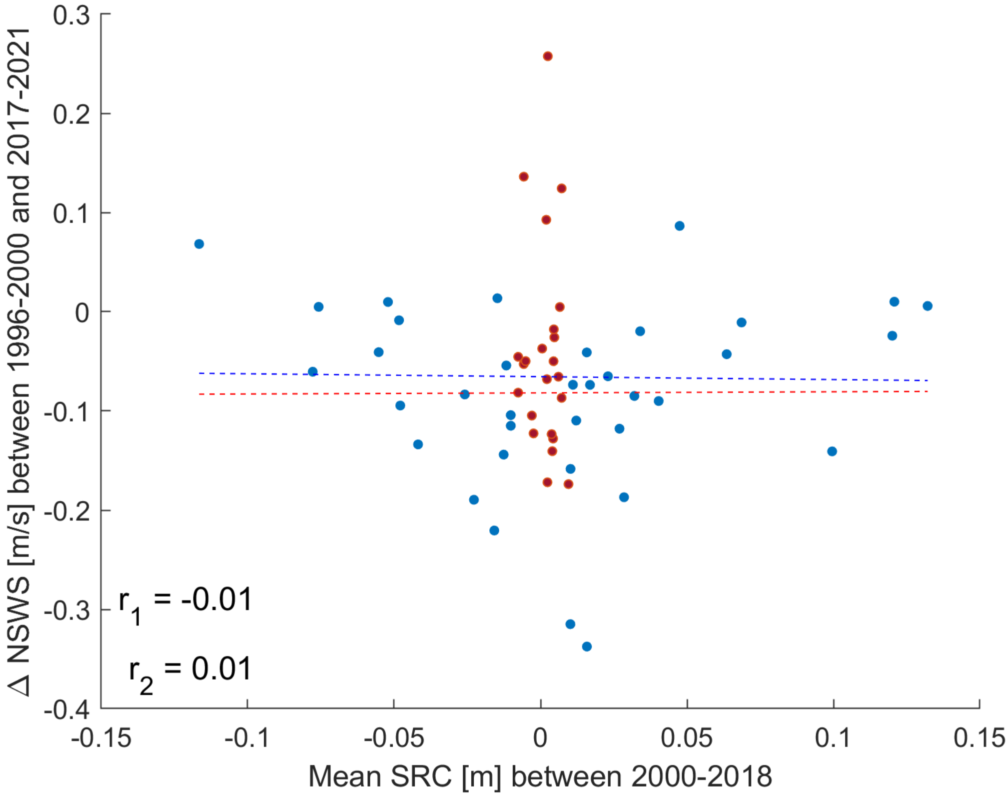

Figure 6: The Relationship of Near-Surface Wind Speed Changes and Surface Roughness Changes. The y-axis shows the difference of the NSWS ratio (Period 3 - Period 1), where Period 1 stands for 1996-2000 and Period 3 stands for 2017-2021. The NSWS is the ratio of $\vec{U}_{\text{Observation}}/\vec{U}_{\text{ERA5}}$. The x-axis corresponds to the mean SRC over the measured area. The correlation r_1 includes all data points, while the correlation r_2 is calculated by only including data points whose mean SRC is outside of -0.01 and 0.01 meter (blue data points). The data that does not fulfill that criteria is shown in red.

Figure 6 shows the result of the ODR-methodology or alternatively phrased, how the NSWS might be affected by the SRC, i.e. it measures their relationship. In this context, the first period and third period were used as indicators of change for the NSWS and the second period was utilized as the time frame that induced the potential alterations of the SR. As mentioned in Section 2.2.4, the NSWS displayed the changes of the ratio $\vec{U}_{\text{Observation}}$ divided by $\vec{U}_{\text{Reanalysis}}$. In that sense, the NSWS changes are negative if the ratio decreased in Period 3 compared to Period 1 and vice versa for a potential increase. Because of this method, one should not understand any changes to be the absolute changes of the observational data, but rather as deviations from the Reanalysis data. The changes on the x-axis explain the sign and magnitude of SRC over the course of the inspected time period two. To measure the SRC, this study documented the SRC in the one kilometer radius around each station, calculated its area, the mean change of the surface roughness length in those changed areas and averaged the change over the entirety of the measured area. The higher the mean SRC is, the more unilateral the changes over the considered time frame in each station's proximity. A large decrease in mean SR would thus be considered a rather one-side event where the SR sank, e.g. in a deforestation effort. A positive sign of total SRC could consequently be considered a result of forestation or Urbanization.

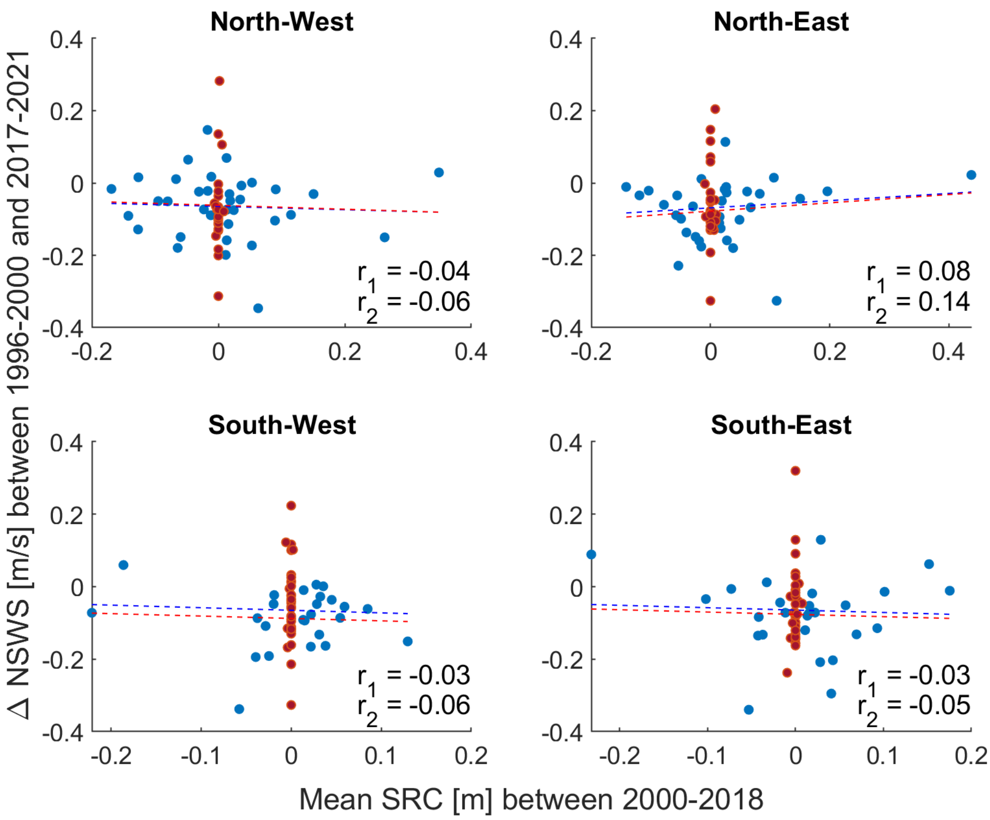

Figure 7: The Relationship of Near-Surface Wind Speed Changes and Surface Roughness Changes when isolating the spatial and directional information of the SRC and NSWS respectively. The y-axis shows the difference of the NSWS ratio (Period 3 - Period 1) in four Directions, where Period 1 stands for 1996-2000 and Period 3 stands for 2017-2021. The NSWS is the ratio of $\vec{U}_{\text{Observation}}/\vec{U}_{\text{ERA5}}$. The x-axis corresponds to the mean SRC in each quadrant's surface area with a 1 km radius. The correlation r_1 includes all data points, while the correlation r_2 is calculated by only including data points whose mean SRC is outside of -0.01 and 0.01 meter (blue data points). The data that does not fulfill that criteria is shown in red.

Focusing on the plotted data itself, this study found that the majority of the 59 stations have shown slightly negative NSWS changes between the first and the third period. These changes were most often between 0 and -0.2 metre per second. At the same time, the mean SRC lied frequently between plus and minus 0.05, but did exceed that limit on multiple occasions. NSWS changes were extremely variable, ranging from over 0.25 to less than -0.35 m s^{-1}, when the mean SRC was close to zero. The overall correlation r_1 was found to be extremely weak at -0.01, and changing sign to 0.01 for r_2. The overall trend when including all data points was found to be $y_1 = -0.0292x - 0.0655$. When excluding the previously mentioned data points of low SRC strength and strong NSWS changes the trend becomes marginally steeper at $y_2 = 0.0110x - 0.0818$. By that measure, one could assume that if the mean SRC was increased by 1 meter, the NSWS should on average decrease by 0.0292 and increase by 0.011 metre per second, respectively.

The subsequent step was to test whether or not the results would become more clear by spatially distinguishing between the SRC and the impact they might induce on the NSWS blowing from these respective directions. Simply put, did NSWS change when isolating its directional vector and lining it up spatially with the SRC?

Figure 7 is indicative that a more distinct relationship between these two variables cannot be found with this method. While the North-West, South-West and South-East directions show a slightly stronger correlation, when excluding data points with close to zero mean SRC, than the relationship shown in Figure 6, with $r_{NW} = -0.06$ and $r_{SW} = -0.06$ and $r_{SE} = -0.05$, the opposite is true for the North-East direction where the correlation switched the sign and a correlation of $r_{NE} = 0.14$ was found, contradicting the information that was found for the other directions. On principle, the slightly increased correlation in the three directions north-West, South-West and South-East does not seem to be significantly better than for Figure 7.

Finally, the change of the mean NSWS over time is displayed in Figure 8. Once again, the differences shown in this Figure are the result of subtracting the mean NSWS of period one of period three (p_3 minus p_1). The plot compares the changes for all 59 stations whose surroundings experienced some significant form of SRC called Observation and the corresponding reanalysis data points called ERA5. A look at the observations with SRC reveals a negative trend. The median value was found to be -0.172 m s^{-1}. The comparison measure, the reanalysis data, showed largely positive trends with a median of 0.049 m s^{-1} for ERA5. Quiet distinctively, the reanalysis data points were matched very closely which can be seen in the range between the 25^{th} (0.024 m s^{-1}) and 75^{th} (0.080 m s^{-1}) percentiles. Additionally, no outliers were found for the reanalysis data. In contrast, the data points of the observations spread wider, although the number of outliers was not considerably higher with three. The range of the 25^{th} and 75^{th} percentiles were larger for the observations at -0.341 m s^{-1} and -0.037 m s^{-1}. When tested against each other with a two-sample t-test, the changes in the ERA5 data points were significantly different to the changes in the observations with $p \ll 0.05$.

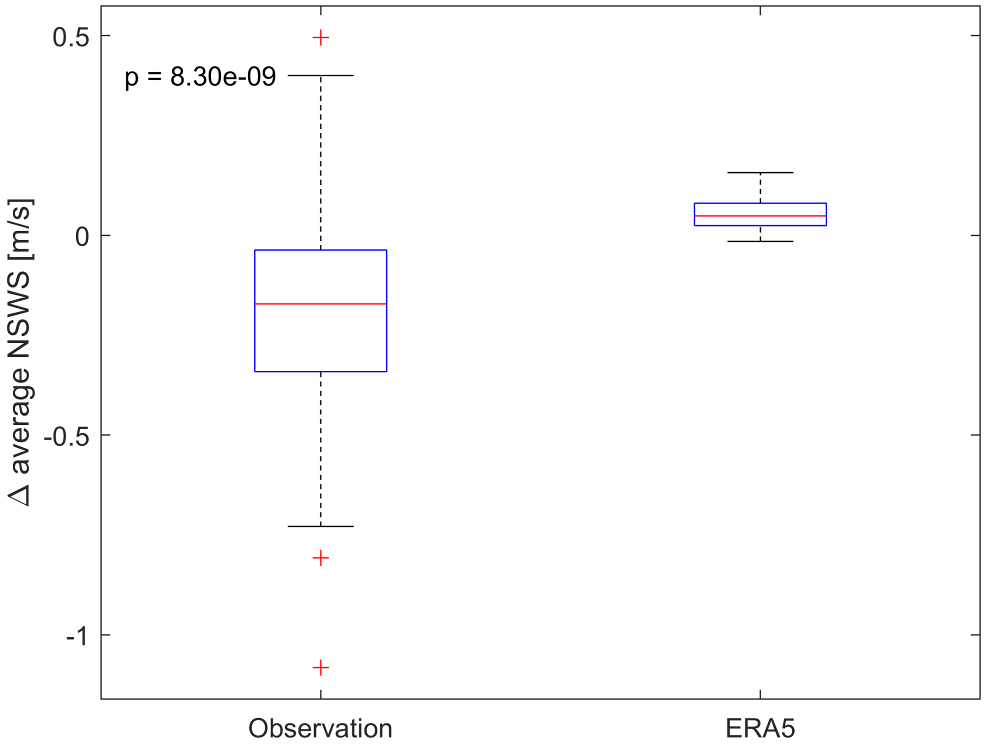

Figure 8: The trends in NSWS changes for the observational data and ERA5. The figure shows the changes for the 59 stations, that experienced SRC between 2000-2018 as well as the changes for the corresponding ERA5 grid points. The y-axis shows the difference in the NSWS (Period 3 - Period 1), where Period 1 stands for 1996-2000 and Period 3 stands for 2017-2021.

4 Discussion

This study pointed out, that Europe has had a complex land cover structure at the start of the documentation and during the beginning of the 21^{st} century until the last documentation in 2018 and that it has undergone large amounts of LULCC. These changes were diverse and almost exclusively found to be on the local and regional scale, most often spanning a few hectares. From time to time, larger changes occurred as a result of natural transition, anthropogenic interference or special events such as wildfires. Despite some categorically clear trends on the national and international level, few areas were found with large uniform signs of change. This is hardly surprising, considering Europe is divided into over forty countries that have their own decision-making processes and priorities for the LU depending on each country's needs, regulations and policies. The bigger picture showed that the vast amount of changes was due to decreases in Agricultural land throughout central Europe and decreases in Shrub & transitional Woodland decreases, especially in Scandinavia and Spain. The largest increases were found to be due to forestation once again in Scandinavia and Spain as well as Urbanization throughout Europe. Importantly, Urbanization in Europe has mainly been found to be due to efforts of extending metropolitan areas, i.e. preexisting cities were enlarged and added to. This trend was found for almost the entirety of Europe except for Bulgaria and Romania. Urban areas have on average lower albedo and less evaporation [T.R. Oke (1982)], due to the artificial LC. Additionally, wind flow and speed are highly disturbed with decreases thereof behind buildings and increases directly to their sides [Mittal et al. (2018), Troen & Petersen (1989)]. The increase of peripheral urban areas, found in this study, is important for future research because urbanized areas are already subject to heat accumulation in the form of the urban heat island effect [Yang et al. (2016)] and endangers the heat-susceptible population. Although dependent on the shared socioeconomic pathway, Gao & O'Neill (2020) estimate future Urbanization in Sweden to be rather low. On the other hand, Swedish forests are likely to undergo heavy management with peak harvesting in the 2030s, as a result of past land management [Blanco et al. (2017)]. Based on their simulations, the authors expect this process to result in vast changes in biodiversity, recreation and carbon sequestration, which go beyond the pure biogeophysical properties of the forests.

In terms of comparability, the LULCC results do not match up not particularly well with previous work on the matter. Zhou et al. (2021) chose to analyze the LULC and subsequent change in Scandinavia between 1992 and 2018 using *European Space Agency climate change initiative land cover products* (ESA-CCI-LC) and *Copernicus Climate Change Service climate data store and land cover products* (C3S-CDS-LC). The authors utilized the former product for the 1992-2015 time frame and the latter product complemented that from 2016 to 2018. Both products have a 300 meter resolution. In principle, the study conducted by Zhou et al. (2021) shows extremely similar results for the original state and the change of Settlements, which are defined as Urban in this study, as well as for the Agriculture and forest areas in Denmark. In contrast, comparing the results for the remaining Scandinavian countries shows that these two studies do not agree well, with consistently higher amounts of Urban and Agricultural areas and lower amounts of forest areas in this study in the original state. Additionally, this study shows comparatively small changes or changes of negative signs for agricultural areas while Zhou et al. (2021) found rather strong increases for this particular group. Similar results were apparent for the Urban/Settlement class. Finally, while this study found strong increases for the Forest classes in Finland and Sweden, Zhou et al. (2021) found almost no change in Finland and a strong decrease in Sweden. More specifically, they found forest areas to have decreased in Sweden by 13 x 10^3 km^2 in said time span from circa 310 x 10^3 km^2 to circa 297 x 10^3 km^2 in 2018. This study in contrast found an opposite trend, with an increase between 2000 and 2018, from roughly 250 x 10^3 km^2 to approximately 262 x 10^3 km^2. According to their study, a large share of this forest decrease was found to be due to an increase in agricultural land, which could not be replicated in this study. In the annual report on the state of the Swedish forests, Nilsson et al. (2022) stated that 279 x 10^3 km^2 forest area existed in 2021. While this study as well as Zhou et al. (2021) differ equally from this mark, Nilsson et al. (2022) also report that the total forest area has decreased between 2003 and 2017 by approximately 2000 km^2. They argue that while the Swedish Forestry sector has increased the density of forests outside of the formally protected areas, the total area was decreased. Although it contradicts the results shown here and raises questions about the origin of the error, it is a type of LUC because it clearly is a sign of changes in the forest management that can potentially increase the shelter effect as described in Section 1.2.

Statistics on Europe's forests were published by Forest Europe (2020), which include the information by Nilsson et al. (2022), but furthermore the rest of Europe. Comparing the forest area per country in 2018 from this study with the information provided on forest area per country in 2020, it becomes visible that the final stages of Europe's forests match up relatively well. All forest changes in Europe combined sum up to approximately 1.73 Million km^2 in this study, while Forest Europe (2020) reports approximately 2.05 Million km^2 for the countries addressed in this study, excluding Malta, Monaco, San Marino and Kosovo, the latter was not documented in their report. Thus, a difference of roughly 278 x 10^3 km^2 was found. In principle, the data compares well, with 26 out of 37 countries being within 20% under or 10% over the reported data for the respective country. A few countries differ quite strongly in forest extent, namely Spain, Turkey and the UK. All of these were underrepresented in this study by 28%, 48% and 36%, respectively. No direct spatial trend was obvious for the outlying countries. Quiet interestingly, when comparing the original state, forest area in 2000, the reported data by *Forest Europe* and the data within this study match up better than in the final stage of reporting, which can be seen in the difference between the two groups at roughly 189 x 10^3 km^2. A major role in these differences in both time frames is arguably the discrepancy within the Turkish data sets of approximately 79 x 10^3 and circa 107 x 10^3 km^2, respectively. Nonetheless, it is apparent that the two data sets differ quite significantly and that the results compare worse over time. This is pretty remarkable considering the validation process by Copernicus [Büttner et al. (2021)], reporting an overall accuracy of $\geq$ 85% for the vector layer.

Finally, the European Environmental Agency (2020) found the forest areas in Europe to be quite stable in the time frame 2000-2018, stating that it grew by 70 km^2 in the 39 considered European countries. Their results tend to vary from both this study and the report by Forest Europe. Especially in the Mediterranean region from Spain to Turkey, Forest Europe (2020) reported strong increases in most countries. On the contrary, European Environmental Agency (2020) did not reproduce these results, showing either deforestation or spatially mixed results. In Eastern Europe, the report by Forest Europe seems to match up better with European Environmental Agency (2020) than this study. Especially Hungary, Poland, the Baltic region and Finland match relatively well. Interestingly, European Environmental Agency (2020) agrees with the increase in forest cover in Sweden that was found in this study, although on a far smaller level.

One explanation for the strong deviation could be the process of Reclassification, described in Section 2.1, which was necessary in order to handle the vast amount of information in these CLC maps, but could at the same time create mismatches with classifications made by Zhou et al. (2021), but seems unlikely to be a reasonable explanation for the discrepancy to the report issued by Forest Europe (2020). Further errors could also be a result of the characterization and definition of Woodland on the national level and at Copernicus, i.e. what canopy size and density does an area have to cover to be classified as a forest or as shrub/transitional woodland. This might also be dependent on the prominent harvesting methods, which may differ at the national level. No information on the classification was found at the time of this study. Furthermore, errors in LULC composition can often be ascribed to imprecise classification, due to the photo-interpretation of the satellite data, where the error rate is strongly linked to the landscape and their estimated classification [Büttner et al. (2021)]; but additionally due to raster format usage, as done in this study. It may lead to spatial bias and or change in the composition of a landscape because the majority of LULC patches are not as large as the pixel size [Schmit et al. (2006)], and thus the more dominant LULC can be determined as the class. This can be especially problematic when the raster resolution is low and transitions between classes occur that show lesser classification certainty [Schmit et al. (2006), Zhou et al. (2021)]. Given the usage of the "cell center method" for the rasterization process of the vector layers, it seems reasonable to assume that strong bias was induced in this step and could explain deviations from previous work on the matter. Furthermore, one of the most frequent transitions in Europe and especially in Sweden was deforestation and forestation from shrub and/or transitional Woodland, which could be less robust depending on the consistency of classification between the CLC-product and the reporting on the national level. Silva et al. (2007) emphasize this point specifically, stating that transitional classes vary significantly from site to site and furthermore that their importance has a tendency to depend on the relief. Finally, the application of satellite data prohibits the distinction between LU and LC [Schmit et al. (2006)], which can lead to unexpected differences in z_0 between two supposedly equal classes, e.g. different growth rates.

One might expect the mean SR to increase over the continent during the study period, because of the increase in urban and forest areas and the decrease in agricultural land and transitional woodland. Considering the spatial and temporal distribution of the changes, these might be stronger in certain areas than others. As this study points out, the impact of the biogeophysical parameters is extremely local and it might thus come down to the small-scale density of SRC within the considered area. Based on the vast amount of forestation in Finland, Sweden and Spain, the chances of SRC increase within these countries and are lower in central Europe. How this impacts the wind speed is not clear, since no correlation between the NSWS and the SRC was found in this study. Past research on the matter, however, would suggest that the NSWS could be slowed down [Minola et al. (2022), Vautard et al. (2010), Wever (2012) and Zha et al. (2019)].

The examination of Sweden indicates a large number of LULCC and consequently SRC, totalling 15.3% of the entire territory. Despite the large number of changes, the mean SRC was found to be consistently low, due to the fact that the changes were averaged over the entire respective region. These numbers occur also as a result of the alterations of opposite signs and subsequent partial offsets. Ultimately, the SRC in Sweden seems to be low overall because the changes apparently cancel each other out. As described before, LULCC do not appear to play a major role on larger scales. On a smaller scale, this effect is very much dependent on the regions' and communities' respective methods of applying changes, e.g. which forest management practice is applied (Thinning, Clear cut or Other)? Because the results of the SRC are strongly dependent on the level of accuracy of the classification process, it is reasonable to assume that the data is affected by uncertainties and errors, considering the disagreement of the LULCC results in this study and comparable reports. Additional errors for the SRC may result from the uncertainties regarding the respective location of each LULC parcel, because depending on the soil and climatic characteristics the species may differ from region to region and thus possess different SR-related characteristics [Silva et al. (2007)], such as canopy height, planting density and canopy size. The latter can influence the availability of sunlight on the ground and thus control the conditions for other species, such as shrubs, to allow or inhibit secondary growth. Silva et al. (2007) ascribed the CLC classes SR values based on the report by Troen & Petersen (1989) and tested them on different sites in Portugal. Despite the uncertainties mentioned above, the authors conclude that the SR values represented their site's roughness "good enough".

Most stations observed a negative trend in NSWS between Period one and three (Figure 8), which was not replicated by their corresponding reanalysis data set, i.e. these data sets were significantly different to their counterparts, which implies that there is some form of change at the observational level, that is not contained in the reanalysis data. This trend agrees with previous work on the matter, as summarized by Wu et al. (2018). Although that specific research states that large-scale circulation patterns are unlikely to be the only influencing factor [Wu et al. (2018)], it is unclear whether or not the differences between the observations and the ERA5 data relate to the SRC in Sweden or if they are due to the large-scale atmospheric circulation changes. The ODR-method was applied for exactly that reason, trying to distinguish between changes in driving force and drag force. While other methods to disentangle these two processes exist, the ODR-method was chosen because it should in theory be able to function regardless of location [Wu et al. (2018)], as long as some form of SRC is applied. As shown in Figure 6 and 7, the relationship between SRC and NSWS seems to be relatively inconclusive. Neither the ODR-method with 360 degree nor the more detailed directional examination showed medium to strong correlations, that resemble the results by Minola et al. (2022).

The absence of clear results in this study is likely attributable to a variety of reasons, such as noise and imprecise representation of the LULCC and therefore the SRC. One case for the latter is not only the above-mentioned deviation from different LULCC reporting but also a very specific comparison to the example shown in the publication by Minola et al. (2022). The authors used orthophotos to manually distinguish between changes in forest cover around their examined wind stations. In their paper, they displayed, as an example, the wind station *Malexander A* as well as its surroundings and the changes thereof. When that very station was investigated in this study, no LULCC/SRC was found using the CLC raster layer. The CLC raster layer likely did not detect the change, because of the size of the area. Thus, the station had not met the criteria of inclusion and was consequently disregarded. It becomes quite apparent, that changes of the LULC at all wind stations can potentially either be neglected although they actually exist or they can be detected despite lacking change in reality. This is a tangible example of the raster issue indicated by Schmit et al. (2006). It would also certainly be an important issue to test in order to understand the error rate for the SRC.

As briefly mentioned in Section 2.2.4, a lack of results can also be attributed to noise in the data, which needs to be disentangled before seeing the actual impact of change in z_0 on the NSWS.

Besides the above-suggested external factors, one could debate whether or not the information was clouded by seasonal variance. Minola et al. (2020) found during their investigation of the ERA5 performance, that the reanalysis product shows a weak bias for seasonal winds, especially found at inland stations. The authors report that ERA5 seems to overestimate the wind conditions by up to 2 m s^{-1} in inland areas and even larger discrepancies were found for mountainous areas. This initial bias is attributable to the differences in how the data sets are assimilated but also to the resolution that the data is based on [Wu et al. (2018)]. It has been shown to influence the results of the ODR-method, which is naturally dependent on the reanalysis data. Secondly, one can assume that the NSWS change is also dependent on the NSWS before encountering the obstacle, that exerts some form of impact on the wind. This logic is derived from the calculation by Troen & Petersen (1989) how the wind speed decreases behind an obstacle. As described in Section 1.2, the strength of this so-called shelter effect depends on different variables, but it ultimately exerts a certain relative reduction of the NSWS. Therefore, the higher the wind speed before encountering the obstacle, the higher the absolute reduction. Considering the wind speed distribution found across all stations in this study, displayed in Figure 5, it is reasonable to assume that the vast amount of measurements ≤ 3 m s^{-1} might have contributed to the noise.

This study shows clearly that analysing the effects of LULCC on the climate, especially on the wind, is heavily dependent on the accuracy of the utilized data. A lack thereof has likely been responsible for errors and uncertainties for the LULCC in Europe and Sweden, which ultimately created noise, clouding definitive results for the NSWS. It was additionally limited by the data availability. In the field of Atmospheric Science and Climatology, it is often emphasised to include data sets of at least 20 to 30 years in order to understand interdecadal variations. Because of the scarce information base, as described in Section 2.1, it is only possible to cover the time period of 2000 until 2018 for the LULCC and the time period 1996 - 2021 for the NSWS. Consequently, this has not been an attempt to understand these long term variations, but rather if the LULCC has an effect on the NSWS on shorter time spans. In terms of methodology, it seems less likely that the chosen ODR-methodology is responsible for the inaccuracy in the NSWS analysis, instead the impact of the raster usage and its spatial bias induced noise early on. Given the bias of LULCC in raster layers, a real time experiment where the NSWS is measured sufficiently long before and after an accompanied LULCC should give clarity. That said, it is unlikely that future work can focus on in-situ measurements at least within the short term, because any examination of climate-related variables needs a strong temporal foundation, i.e. data sets of the climate variable have to be several years long before and after the to be inspected effect. It is therefore recommended to intensify the focus on the parameterisation of previous LULCC, in order to tell apart any changes from the spatial bias, which seems to be the major reason for the lack of clarity. This process could be initiated by using the vector layers, which should provide information of higher quality. The downside is that these layers contain comparatively sizeable amounts of data and processing is hampered. Further work should additionally try to mitigate the effect of seasonal variance and its bias on the NSWS when applying the ODR-method. Previous work has also shown that numerical modeling can be an effective measure to analyse the LULCC impact on NSWS [Zha et al. (2019)]. Finally, while this study tried to find out if the NSWS is significantly influenced by LULCC generally, it did not cover the effect on wind gusts. These could have been more predominately affected and isolating stronger wind speeds, might clarify any noise that is being ignored when using the entirety of the wind data.

5 Conclusion

This study intended to identify and understand the alterations of Land use and Land cover in Europe for the start of the 21st century, using the CLC raster layer maps provided by Copernicus and subsequently determine whether or not these alterations would affect the NSWS in Sweden. LULCC were found across Europe and especially in Sweden, with strong signs of forestation. No relation between the NSWS and the LULCC became apparent in this context, despite the attempt of isolating the effect of surface roughness, utilizing observational and reanalysis data with the ODR-method. This study has furthermore focused on aligning the two components spatially, which did not improve the results significantly.

When addressing the effects of LULCC on NSWS, the majority of preceding publications relied on observational data. In the process, these studies found varying correlations and influences, respectively, between the aforementioned LULCC and NSWS changes. This study tried to initiate the ODR-method in Sweden using observational and ERA5 data, to tackle how strong the effect of LULCC induced alterations of the surface roughness length is on the the wind. This methodology could not confirm the previously found results, probably owing to the above-mentioned spatial bias of the LULCC. This raises the question if other methodologies are generally better suited for this purpose or if it just comes down to eradicating inaccuracies, errors and noise.

It is thus essential to tackle that question further, focusing on clearing up noise created by seasonal variance and slow wind, but more importantly, adding to mitigating the effect of LULCC bias induced by the raster usage. That is especially crucial because it serves as the foundation of any LULCC related work and could therefore heavily influence the results when working with climatic variables. Numerical modelling may also be helpful in reducing the noises involved.

6 References

[1] Ahlswede, B. J. and Thomas, R. Q. (2017). Community earth system model simulations reveal the relative importance of afforestation and forest management to surface temperature in Eastern North America. *Forests*, 8(12):–.

[2] Alkama, R. and Cescatti, A. (2016). Biophysical climate impacts of recent changes in global forest cover. *Science*, 351(6273):600–604.

[3] Andreas, E. L., Claffy, K. J., Jordan, R. E., Fairall, C. W., Guest, P. S., Persson, P. O. G., and Grachev, A. A. (2006). Evaluations of the von Karman constant in the atmospheric surface layer. *Journal of Fluid Mechanics*, 559:117–149.

[4] Arora, V. K. and Montenegro, A. (2011). Small temperature benefits provided by realistic afforestation efforts. *Nature Geoscience*, 4(8):514–518.

[5] Blanco, V., Holzhauer, S., Brown, C., Lagergren, F., Vulturius, G., Lindeskog, M., and Rounsevell, M. D. (2017). The effect of forest owner decision-making, climatic change and societal demands on land-use change and ecosystem service provision in Sweden. *Ecosystem Services*, 23:174–208.

[6] Boisier, J. P., De Noblet-Ducoudré, N., Pitman, A. J., Cruz, F. T., Delire, C., Van Den Hurk, B. J., Van Der Molen, M. K., Mller, C., and Voldoire, A. (2012). Attributing the impacts of land-cover changes in temperate regions on surface temperature and heat fluxes to specific causes: Results from the first LUCID set of simulations. *Journal of Geophysical Research Atmospheres*, 117(12).

[7] Bonan, G. B. (2008). Forests and Climate Change: Forcings, Feedbacks, and the Climate Benefits of Forests. *Science*, 320(5882):1444–1449.

[8] Bright, R. M., Davin, E., O'Halloran, T., Pongratz, J., Zhao, K., and Cescatti, A. (2017). Local temperature response to land cover and management change driven by non-radiative processes. *Nature Climate Change*, 7(4):296–302.

[9] Bright, R. M., Zhao, K., Jackson, R. B., and Cherubini, F. (2015). Quantifying surface albedo and other direct biogeophysical climate forcings of forestry activities. *Global Change Biology*, 21(9):3246–3266.

[10] Büttner, G., Kosztra, B., Maucha, G., Pataki, R., Kleeschulte, S., Hazeu, G., Vittek, M., and Littkopf, A. (2021). Copernicus land monitoring service - corine land cover user manual. Technical Report 1, European Environment Agency.

[11] Cohn, A. S., Bhattarai, N., Campolo, J., Crompton, O., Dralle, D., Duncan, J., and Thompson, S. (2019). Forest loss in Brazil increases maximum temperatures within 50 km. *Environmental Research Letters*, 14(8):–.

[12] Copernicus (2023). Corine land cover. https://land.copernicus.eu/pan-european/corine-land-cover. (Accessed on 23-Mar-2023).

[13] Davin, E. L., Rechid, D., Breil, M., Cardoso, R. M., Coppola, E., Hoffmann, P., Jach, L. L., Katragkou, E., De Noblet-Ducoudré, N., Radtke, K., Raffa, M., Soares, P. M., Sofiadis, G., Strada, S., Strandberg, G., Tölle, M. H., Warrach-Sagi, K., and Wulfmeyer, V. (2020). Biogeophysical impacts of forestation in Europe: First results from the LUCAS (Land Use and Climate across Scales) regional climate model intercomparison. *Earth System Dynamics*, 11(1):183–200.

[14] Devaraju, N., De Noblet-Ducoudré, N., Quesada, B., and Bala, G. (2018). Quantifying the Relative Importance of Direct and Indirect Biophysical Effects of Deforestation on Surface Temperature and Teleconnections. *Journal of Climate*, 31(10):3811–3829.

[15] Devasthale, A., Carlund, T., and Karlsson, K. G. (2022). Recent trends in the agrometeorological climate variables over Scandinavia. *Agricultural and Forest Meteorology*, 316.

[16] ECMWF (2023a). Energy fluxes - land - htessel. https://confluence.ecmwf.int/display/FUG/Energy+Fluxes+-+Land+-+HTESSEL. (Accessed on 12-Jun-2023).

[17] ECMWF (2023b). Era5: How to calculate wind speed and wind direction from u and v components of the wind? https://confluence.ecmwf.int/pages/viewpage.action?pageId=133262398. (Accessed on 23-Mar-2023).

[18] EEA (2020). Land cover accounts: an approach to geospatial environmental accounting. Technical Report 12/2020, European Environment Agency, Publications Office.

[19] Frauenfeld, O. W., Zhang, T., and Serreze, M. C. (2005). Climate change and variability using European Centre for Medium-Range Weather Forecasts reanalysis (ERA-40) temperatures on the Tibetan Plateau. *Journal of Geophysical Research D: Atmospheres*, 110(2):1–9.

[20] Gao, J. and O'Neill, B. (2020). Mapping global urban land for the 21st century with data-driven simulations and shared socioeconomic pathways. *Nature Communications*, 11(2302).

[21] Hagemann, S. (2002). An improved land surface parameter dataset for global and regional climate models. Technical Report 336, Max Planck Institute for Meteorology.

[22] Hersbach, H., Bell, B., Berrisford, P., Biavati, G., Horányi, A., Muñoz Sabater, J., Nicolas, J., Peubey, C., Radu, R., Rozum, I., Schepers, D., Simmons, A., Soci, C., Dee, D., and Thépaut, J.-N. (2023). Era5 hourly data on single levels from 1940 to present. https://cds.climate.copernicus.eu/cdsapp!/dataset/reanalysis-era5-single-levels?tab=form. (Accessed on 23-Mar-2023).

[23] Hersbach, H., Bell, B., Berrisford, P., Hirahara, S., Horányi, A., Muñoz-Sabater, J., Nicolas, J., Peubey, C., Radu, R., Schepers, D., Simmons, A., Soci, C., Abdalla, S., Abellan, X., Balsamo, G., Bechtold, P., Biavati, G., Bidlot, J., Bonavita, M., De Chiara, G., Dahlgren, P., Dee, D., Diamantakis, M., Dragani, R., Flemming, J., Forbes, R., Fuentes, M., Geer, A., Haimberger, L., Healy, S., Hogan, R. J., Hólm, E., Janisková, M., Keeley, S., Laloyaux, P., Lopez, P., Lupu, C., Radnoti, G., de Rosnay, P., Rozum, I., Vamborg, F., Villaume, S., and Thépaut, J. N. (2020). The ERA5 global reanalysis. *Quarterly Journal of the Royal Meteorological Society*, 146(730):1999–2049.

[24] Hickey, R. J. (1996). Noise modelling and evaluating learning from examples. *Artificial Intelligence*, 82(1-2):157–179.

[25] Hirsch, A. L., Wilhelm, M., Davin, E. L., Thiery, W., and Seneviratne, S. I. (2017). Can climate-effective land management reduce regional warming?. *Journal of Geophysical Research*, 122(4):2269–2288.

[26] Jia, G., E. Shevliakova, P. Artaxo, N. De Noblet-Ducoudré, R. Houghton, J. House, K. Kitajima, C. Lennard, A. Popp, A. Sirin, R. Sukumar, L. Verchot, P.R. Shukla, J. Skea, E. Calvo Buendia, V. Masson-Delmotte, H.-O. Pörtner, D.C. Roberts, P. Zhai, R. Slade, S. Connors, R. van Diemen, M. Ferrat, E. Haughey, S. Luz, S. Neogi, M. Pathak, J. Petzold, J. Portugal Pereira, P. Vyas, E. Huntley, K. Kissick, M. Belkacemi, and J. Malley (2019). Land–climate interactions. in: Climate change and land: an ipcc special report on climate change, desertification, land degradation, sustainable land management, food security, and greenhouse gas fluxes in terrestrial ecosystems. Technical report, IPCC, Cambridge, United Kingdom and New York, NY, USA.

[27] Kalnay, E. and Cai, M. (2003). Impact of urbanization and land-use change on climate.. *Nature*, 423(6939):528–531.

[28] Kosztra, B. and Büttner, G. (2019). Updated clc illustrated nomenclature guidelines. Technical report, European Environment Agency, Wien, Austria.

[29] Lambin, E. F., Turner, B. L., Geist, H. J., Agbola, S. B., Angelsen, A., Bruce, J. W., Coomes, O. T., Dirzo, R., Unther Fischer, G. U., Folke, C., George, P. S., Homewood, K., Imbernon, J., Leemans, R., Li, X., Moran, E. F., Mortimore, M., Ramakrishnan, P. S., Richards, J. F., Sk, H., Steffen, W., Stone, G. D., Svedin, U., Veldkamp, T. A., Vogel, C., and Xu, J. (2001). The causes of land-use and land-cover change: moving beyond the myths. *Global Environmental Change*, 11(4):261–269.

[30] Lejeune, Q., Davin, E. L., Gudmundsson, L., Winckler, J., and Seneviratne, S. I. (2018). Historical deforestation locally increased the intensity of hot days in northern mid-latitudes. *Nature Climate Change*, 8(5):386–390.

[31] Li, Y., Wang, Y., Chu, H., and Tang, J. (2008). The climate influence of anthropogenic land-use changes on near-surface wind energy potential in China. *Chinese Science Bulletin*, 53(18):2859–2866.

[32] Liao, W., Liu, X., Burakowski, E., Wang, L., Li, D., and Wang, L. (2020). Sensitivities and Responses of Land Surface Temperature to Deforestation-Induced Biophysical Changes in Two Global Earth System Models. *Journal of Climate*, 33(19):8381–8399.

[33] Liao, W., Rigden, A. J., and Li, D. (2018). Attribution of Local Temperature Response to Deforestation. *Journal of Geophysical Research: Biogeosciences*, 123(5):1572–1587.

[34] Luu, L. N., Meijgaard, E. V., Philip, S. Y., Kew, S. F., De Baar, J. H. S., Stepek, A., Van Meijgaard, E., and De 3 Baar, J. H. S. (2023). Impact of Surface Roughness Changes on Surface Wind Speed over Western Europe: A Study with a Regional Climate Model.

[35] Luyssaert, S., Jammet, M., Stoy, P. C., Estel, S., Pongratz, J., Ceschia, E., Churkina, G., Don, A., Erb, K., Ferlicoq, M., Gielen, B., Grünwald, T., Houghton, R. A., Klumpp, K., Knohl, A., Kolb, T., Kuemmerle, T., Laurila, T., Lohila, A., Loustau, D., McGrath, M. J., Meyfroidt, P., Moors, E. J., Naudts, K., Novick, K., Otto, J., Pilegaard, K., Pio, C. A., Rambal, S., Rebmann, C., Ryder, J., Suyker, A. E., Varlagin, A., Wattenbach, M., and Dolman, A. J. (2014). Land management and land-cover change have impacts of similar magnitude on surface temperature. *Nature Climate Change*, 4(5):389–393.

[36] Masson-Delmotte, V., P. Zhai, A. Pirani, S.L. Connors, C. Péan, S. Berger, N. Caud, Y. Chen, L. Goldfarb, M.I. Gomis, M. Huang, K. Leitzell, E. Lonnoy, J.B.R. Matthews, T.K. Maycock, T. Waterfield, O. Yelekçi, R. Yu, and B. Zhou (eds.) (2021). Climate change 2021: The physical science basis. contribution of working group i to the sixth assessment report of the intergovernmental panel on climate change. Technical report, IPCC, Cambridge, United Kingdom and New York, NY, USA.

[37] McVicar, T. R., Roderick, M. L., Donohue, R. J., Li, L. T., Van Niel, T. G., Thomas, A., Grieser, J., Jhajharia, D., Himri, Y., Mahowald, N. M., Mescherskaya, A. V., Kruger, A. C., Rehman, S., and Dinpashoh, Y. (2012). Global review and synthesis of trends in observed terrestrial near-surface wind speeds: Implications for evaporation. *Journal of Hydrology*, 416-417:182–205.

[38] Minola, L., Reese, H., Lai, H. W., Azorin-Molina, C., Guijarro, J. A., Son, S. W., and Chen, D. (2022). Wind stilling-reversal across Sweden: The impact of land-use and large-scale atmospheric circulation changes. *International Journal of Climatology*, 42(2):1049–1071.

[39] Minola, L., Zhang, F., Azorin-Molina, C., Pirooz, A. S., Flay, R. G. J., Hersbach, H., and Chen, D. (2020). Near-surface mean and gust wind speeds in ERA5 across Sweden: towards an improved gust parametrization. *Climate Dynamics*, 55(3-4):887–907.

[40] Mittal, H., Sharma, A., and Gairola, A. (2018). A review on the study of urban wind at the pedestrian level around buildings. *Journal of Building Engineering*, 18:154–163.

[41] Natural-Earth (2023). 1:10m cultural vectors. https://www.naturalearthdata.com/downloads/10m-cultural-vectors/. (Accessed on 23-Mar-2023).

[42] Nilsson, P., Roberge, C., Dahlgren, J., and Fridman, J. (2022). Skogsdata 2022. tema: Den formellt skyddade skogen. Technical report, Sveriges Lantbruksuniversitet, Umeå.

[43] Oke, T. R. (1982). The energetic basis of the urban heat island. *Quarterly journal of the royal meteorological society*, 108(455):1–24.

[44] Oke, T. R. (1987). *Boundary Layer Climates*. Routledge.

[45] Prins, K. (2020). State of europe's forests 2020. Technical report, Forest Europe.

[46] Quesada, B., Arneth, A., and De Noblet-Ducoudré, N. (2017). Atmospheric, radiative, and hydrologic effects of future land use and land cover changes: A global and multimodel climate picture. *Journal of Geophysical Research*, 122(10):5113–5131.

[47] Ribeiro Wood Thilsted, C., Silva, J., Ribeiro, C., and Guedes (2007). Roughness length classification of corine land cover classes. Technical report.

[48] Schmit, C., Rounsevell, M. D., and La Jeunesse, I. (2006). The limitations of spatial land use data in environmental analysis. *Journal of Climate*, 9(2):174–188.

[49] SMHI (2023). Ladda ner meteorologiska observationer. https://www.smhi.se/data/meteorologi/ladda-ner-meteorologiska-observationerparam=wind,stations=core. (Accessed on 23-Mar-2023).

[50] Sofiadis, G., Katragkou, E., Davin, E. L., Rechid, D., De Noblet-Ducoudre, N., Breil, M., Cardoso, R. M., Hoffmann, P., Jach, L., Meier, R., Mooney, P. A., Soares, P. M., Strada, S., Tölle, M. H., and Warrach Sagi, K. (2022). Afforestation impact on soil temperature in regional climate model simulations over Europe. *Geoscientific Model Development*, 15(2):595–616.

[51] Sorbjan, Z. (1989). *Structure of the atmospheric boundary layer.* Prentice Hall.

[52] Stephens, G. L., O'Brien, D., Webster, P. J., Pilewski, P., Kato, S., and Li, J. L. (2015). The albedo of earth. *Reviews of Geophysics*, 53(1):141–163.

[53] Strandberg, G. and Kjellström, E. (2019). Climate impacts from afforestation and deforestation in Europe. *Earth Interactions*, 23(1):1–27.

[54] Tölle, M. H., Breil, M., Radtke, K., and Panitz, H. J. (2018). Sensitivity of european temperature to albedo parameterization in the regional climate model COSMO-CLM linked to extreme land use changes. *Frontiers in Environmental Science*, 6:123.

[55] Troen, I. E. L. P. and Lundtang Petersen, E. (1989). European wind atlas. Technical report, Risø National Laboratory.

[56] Vautard, R., Cattiaux, J., Yiou, P., Thépaut, J. N., and Ciais, P. (2010). Northern Hemisphere atmospheric stilling partly attributed to an increase in surface roughness. *Nature Geoscience*, 3(11):756–761.

[57] Wever, N. (2012). Quantifying trends in surface roughness and the effect on surface wind speed observations. *Journal of Geophysical Research: Atmospheres*, 117(11).

[58] Wu, J., Zha, J., Zhao, D., and Yang, Q. (2018). Changes in terrestrial near-surface wind speed and their possible causes: an overview. *Climate Dynamics*, 51(5-6):2039–2078.

[59] Yang, L., Qian, F., Song, D.-X., and Zheng, K.-J. (2016). Research on urban heat-island effect. *Procedia Engineering*, 169:11–18. Fourth International Conference on Countermeasures to Urban Heat Island, 30-31 May and 1 June 2016.

[60] Zeng, Z., Wang, D., Yang, L., Wu, J., Ziegler, A. D., Liu, M., Ciais, P., Searchinger, T. D., Yang, Z. L., Chen, D., Chen, A., Li, L. Z., Piao, S., Taylor, D., Cai, X., Pan, M., Peng, L., Lin, P., Gower, D., Feng, Y., Zheng, C., Guan, K., Lian, X., Wang, T., Wang, L., Jeong, S. J., Wei, Z., Sheffield, J., Caylor, K., and Wood, E. F. (2021). Deforestation-induced warming over tropical mountain regions regulated by elevation. *Nature Geoscience*, 14(1):23–29.

[61] Zha, J., Zhao, D., Wu, J., and Zhang, P. (2019). Numerical simulation of the effects of land use and cover change on the near-surface wind speed over eastern china. *Climate Dynamics*, 53:1783–1803.

[62] Zhou, L., Dickinson, R. E., Tian, Y., Fang, J., Li, Q., Kaufmann, R. K., Tucker, C. J., and Myneni, R. B. (2004). Evidence for a significant urbanization effect on climate in China. 101(26):9540–9544.

[63] Zhou, N., Hu, X., Byskov, I., Næss, J. S., Wu, Q., Zhao, W., and Cherubini, F. (2021). Overview of recent land cover changes, forest harvest areas, and soil erosion trends in Nordic countries. *Geography and Sustainability*, 2(3):163–174.

A Appendix - Figures

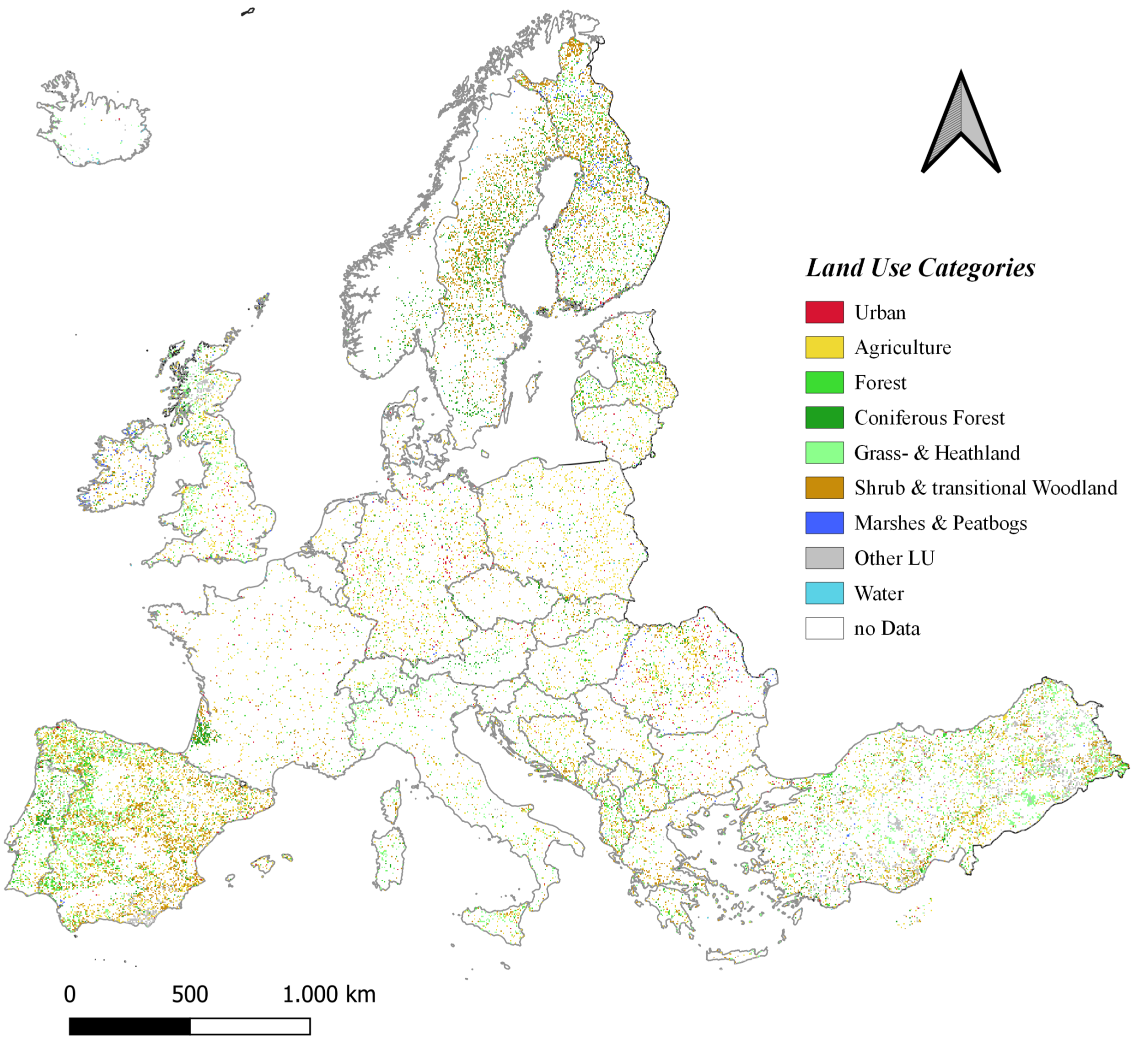

Figure 9: Land Use and Land Cover Changes in Europe between 2000 and 2018. The changes displayed correspond to the LULC that could be found before the alteration. The resolution is set at five km.

B Appendix - Tables

Table 5: Land Use and Land Cover for each country and class in the year 2000 in km^2. The countries displayed correspond to how they exist today and not to the year 2000. Therefore this study distinguishes between Serbia, Kosovo and Montenegro. The classes displayed in this Table correspond to the reclassified classes shown in Table 8.

Country	Urban	Agriculture	Forest	Coniferous forest	Grassland	Shrub	Peatbogs	Other LU	Water
Albania	490.3	8113.7	6641.9	949.4	3062.3	6676.8	40.4	1714.5	646.3
Andorra	0.0	16.3	4.7	60.1	54.0	8.3	0.0	89.0	0.0
Austria	4018.2	27141.7	15276.0	22054.8	8501.8	83.1	235.8	5960.9	720.9
Belgium	6264.8	17627.0	4696.3	1376.9	180.3	164.2	78.1	16.8	265.3
Bosnia & Herzegovina	701.6	18996.7	20435.0	2454.6	2779.9	5339.2	61.4	701.1	357.1
Bulgaria	5478.9	58054.2	29981.0	5433.8	4312.9	7543.7	198.6	576.1	1181.7
Croatia	1535.8	22455.5	19098.1	979.9	2390.1	6763.9	179.2	624.1	996.9
Czechia	4901.3	45130.7	8914.0	17079.8	289.0	1780.6	101.1	2.3	559.5
Denmark	2911.8	32377.3	1947.8	1772.5	815.2	821.4	526.5	51.3	1473.0
Estonia	870.8	14735.4	12695.5	8216.4	446.6	4009.2	1918.5	35.0	2847.3
Finland	4498.3	28896.6	94591.6	98462.2	4147.1	47136.1	22403.1	1070.4	32667.8
France	26833.7	328221.5	107427.0	35464.1	16950.0	17944.5	807.4	8976.7	5217.6
Germany	28927.8	213769.7	47743.4	56178.3	2392.5	2091.5	1371.1	702.6	4497.5
Greece	2737.4	52262.4	16483.8	7231.8	12306.1	34750.3	239.6	2307.4	3033.5
Hungary	5458.1	63039.1	16372.4	1001.8	2274.3	2424.8	856.8	23.2	1748.7
Iceland	301.0	2400.8	297.2	16.7	38394.8	220.7	6727.3	50643.0	3389.2
Ireland	1335.7	46727.2	574.2	2334.3	1415.9	3625.3	11184.5	397.7	1851.2
Italy	14141.9	155570.3	67349.3	12835.6	16459.9	20560.1	168.6	10122.8	3977.1
Kosovo	247.9	4431.1	4009.6	226.8	786.1	1009.0	0.0	178.4	24.3
Latvia	849.4	28337.0	17532.3	9386.2	54.2	5421.7	1547.0	41.8	1386.8
Liechtenstein	19.1	39.5	36.9	13.0	20.8	0.0	0.0	4.8	3.3
Lithuania	2115.5	39810.5	11467.3	7358.4	43.8	2210.2	582.9	29.2	1309.9
Luxembourg	229.9	1436.9	792.0	116.7	1.8	25.9	0.0	0.0	5.1
Malta	89.6	156.1	1.4	0.7	0.0	41.3	0.0	3.4	33.2
Monaco	8.8	0.7	1.6	0.2	1.3	5.3	0.0	0.0	0.8
Montenegro	137.5	2248.1	4629.7	982.5	1304.5	3259.2	109.5	776.4	280.2
Netherlands	4480.0	24986.2	1518.6	1610.2	737.0	15.4	388.5	88.9	3278.1
North Macedonia	379.1	9495.1	8122.1	443.3	1886.8	4399.7	17.7	87.3	554.0
Norway	2175.6	15615.9	45740.7	59089.2	45755.3	5444.6	21063.1	103393.4	21000.3
Poland	12447.1	196606.2	38316.9	55825.2	441.2	3055.9	1075.7	187.9	5028.6
Portugal	2927.4	37280.3	23227.2	7177.6	5159.8	12405.1	65.3	1641.9	1499.0
Romania	14890.9	134500.0	58338.6	11171.8	4194.9	5999.3	3697.5	492.4	3048.6
San Marino	6.8	41.7	6.5	0.0	0.8	4.4	0.0	0.0	0.0
Serbia	2570.8	44155.1	22102.9	865.5	2050.1	4534.6	228.5	207.6	913.4
Slovakia	2642.8	23571.9	14519.3	5220.5	411.1	1683.1	29.2	104.0	275.4
Slovenia	552.9	6974.4	9042.6	2467.7	429.4	452.8	24.5	288.3	93.8
Spain	8155.5	229877.5	77657.5	39827.6	35689.4	98111.5	549.4	12347.0	4659.4
Sweden	5808.2	39027.2	35896.1	214183.5	28850.4	44187.0	28800.5	10372.7	39053.6
Switzerland	2699.4	11801.9	6164.9	6365.3	5594.2	158.5	37.1	7188.9	1425.3
Turkey	11945.8	331743.9	71055.0	47422.3	91171.8	84354.2	2078.1	124956.8	14460.6
United Kingdom	17858.5	142193.4	7095.0	12634.2	48098.6	1909.8	5272.7	4183.2	4534.2

Table 6: Effective Land Use and Land Cover Change for each country and class in km^2. Negative numbers equate to a decrease in the respective class and country. At the same time, a positive number describes an increase. The classes displayed in this Table correspond to the reclassified classes shown in Table 8.

Country	Urban	Agriculture	Forest	Coniferous Forest	Grassland	Shrub	Peatbogs	Other	Water
Albania	278.4	-116.5	-462.3	-141.8	155.9	43.2	3.5	177.2	62.5
Andorra	0.0	-1.2	0.7	0.6	5.9	-4.5	0.0	-1.6	0.1
Austria	953.8	-443.6	-163.7	-548.7	-283.5	460.1	-12.9	22.5	16.0
Belgium	142.7	-154.2	29.1	-44.3	-6.6	23.9	8.1	-4.0	5.3
Bosnia & Herzegovina	183.6	-1864.9	971.9	39.4	422.9	-168.0	5.2	404.0	5.9
Bulgaria	-139.9	61.8	-142.5	-71.9	69.8	234.7	-46.9	-37.3	72.2
Croatia	431.5	-328.8	-435.7	-62.7	-25.0	412.7	2.5	-3.2	8.7
Czechia	331.9	-429.1	280.2	-308.8	-0.4	100.3	2.2	2.6	21.2
Denmark	425.8	-994.4	181.3	-127.4	4.0	453.2	8.1	5.5	44.0
Estonia	97.5	-433.1	421.8	-160.8	-85.4	21.9	133.1	-4.1	9.0
Finland	16.7	-1349.9	7375.3	10981.5	2789.0	-19821.4	-1153.3	681.8	480.3
France	5478.0	-5094.9	2246.6	-1913.1	-228.2	-939.6	27.7	130.0	293.5
Germany	4656.5	-9062.3	2984.6	1263.4	289.1	186.9	-227.7	-427.4	337.0
Greece	1338.9	-1540.2	2367.0	211.0	-2008.0	-1601.1	-11.6	994.5	249.5
Hungary	529.5	-2469.8	164.4	-103.2	25.7	1811.9	5.2	5.2	31.2
Iceland	59.6	134.7	200.2	19.4	-530.8	130.5	-75.5	69.4	-7.4
Ireland	281.5	272.0	605.9	1009.9	-92.8	-1455.3	-1013.2	455.7	-63.7
Italy	2091.0	-1090.4	585.4	-14.1	-6838.0	-754.4	24.8	5888.3	107.4
Kosovo	259.9	-271.7	41.0	-5.1	-9.0	-52.3	1.3	35.6	0.3
Latvia	470.4	-2730.9	-1468.8	-1274.9	32.9	4790.0	51.5	13.3	116.6
Liechtenstein	2.8	-7.3	1.9	6.5	-3.8	0.4	0.8	-1.2	-0.2
Lithuania	84.1	-1707.5	703.7	-9.6	13.9	882.6	-18.0	7.6	43.2
Luxembourg	46.4	-58.0	27.6	3.2	-1.8	-17.9	0.4	0.0	0.0
Malta	1.0	0.6	0.0	0.0	0.0	-1.0	0.0	-0.1	-0.3
Monaco	0.1	0.0	-0.1	0.4	0.0	-0.4	0.0	0.0	0.0
Montenegro	115.9	-65.6	41.1	-10.6	-282.8	-227.8	-3.7	430.6	2.8
Netherlands	873.7	-1255.3	45.4	-29.0	205.7	19.2	99.3	-8.4	49.4
North Macedonia	81.9	-369.8	-455.6	-14.5	276.0	338.7	3.5	124.4	15.3
Norway	269.0	-41.3	51.2	-1496.7	97.7	1138.0	-15.2	3.9	-6.7
Poland	6877.6	-12883.0	2526.5	703.6	-91.6	2682.5	31.9	-39.9	192.3
Portugal	634.9	-1319.7	-3196.8	-2604.7	534.4	6037.7	4.9	-366.6	276.0
Romania	-1725.3	394.6	1711.4	-204.6	2328.1	-1507.5	-917.5	-188.4	109.1
San Marino	1.7	-1.3	-0.5	0.0	-0.4	0.5	0.0	0.0	0.0
Serbia	357.3	-1627.1	251.5	68.7	-40.5	899.4	64.8	-3.9	29.9
Slovakia	316.1	-616.9	840.8	-352.5	-10.3	-207.2	8.7	7.1	14.2
Slovenia	160.8	-127.1	-2.9	-38.5	-39.1	43.4	0.2	-6.6	9.7
Spain	4549.5	-10742.4	8453.6	6920.8	18314.0	-26106.5	-104.2	-1563.4	278.6
Sweden	594.8	306.8	6640.3	5507.5	87.5	-14045.5	1295.6	231.5	-618.5
Switzerland	146.8	-422.1	-151.0	-510.6	-77.6	1116.4	16.7	-122.5	3.9
Turkey	3413.8	8356.5	-4977.1	1476.8	-984.1	3562.0	92.6	-12143.8	1203.4
United Kingdom	3282.9	-6458.7	1069.3	-489.4	-252.4	1883.4	2042.3	-1344.1	266.8

Table 7: Land Use and Land Cover Categories and their corresponding Raster values, Description number as defined by Copernicus. The three columns on the right display the Surface Roughness length Minimum, Maximum and most likely Value, as defined by Silva et al. (2007)

Raster Value	**Description No.**	**Land Use and Land Cover**	**SR Min**	**SR Max**	**SR most likely**
1	111	Continuous urban fabric	1.1	1.3	1.2
2	112	Discontinuous urban fabric	0.3	0.5	0.5
3	121	Industrial or commercial units	0.3	0.5	0.5
4	122	Road and rail networks and associated land	0.05	0.1	0.075
5	123	Port areas	0.3	0.5	0.5
6	124	Airports	-	-	0.005
7	131	Mineral extraction sites	-	-	0.005
8	132	Dump sites	-	-	0.005
9	133	Construction sites	0.3	0.5	0.5
10	141	Green urban areas	0.5	0.6	0.6
11	142	Sport and leisure facilities	0.3	0.5	0.5
12	211	Non-irrigated arable land	-	-	0.05
13	212	Permanently irrigated land	-	-	0.05
14	213	Rice fields	-	-	0.05
15	221	Vineyards	0.1	0.3	0.1
16	222	Fruit trees and berry plantations	0.1	0.3	0.1
17	223	Olive groves	0.1	0.3	0.1
18	231	Pastures	0.03	0.1	0.03
19	241	Annual crops associated with permanent crops	0.1	0.3	0.1
20	242	Complex cultivation patterns	0.1	0.5	0.300
21	243	Land principally occupied by agriculture with significant areas of natural vegetation	0.1	0.5	0.300
22	244	Agro-forestry areas	0.1	0.5	0.300
23	311	Broad-leaved forest	0.6	1.2	0.75
24	312	Coniferous forest	0.6	1.2	0.75
25	313	Mixed forest	0.6	1.2	0.75
26	321	Natural grasslands	0.03	0.1	0.03
27	322	Moors and heathland	0.03	0.1	0.03
28	323	Sclerophyllous vegetation	0.03	0.1	0.03
29	324	Transitional woodland-shrub	0.5	0.6	0.6
30	331	Beaches - dunes - sands	-	-	0.0003
31	332	Bare rocks	-	-	0.005
32	333	Sparsely vegetated areas	-	-	0.005
33	334	Burnt areas	0.5	0.6	0.6
34	335	Glaciers and perpetual snow	-	-	0.001

35	411	Inland marshes	-	-	0.05
36	412	Peat bogs	-	-	0.0005
37	421	Salt marshes	-	-	0.05
38	422	Salines	-	-	0.0005
39	423	Intertidal flats	-	-	0.0005
40	511	Water courses	-	-	0
41	512	Water bodies	-	-	0
42	521	Coastal lagoons	-	-	0
43	522	Estuaries	-	-	0
44	523	Sea and ocean	-	-	0
48	999	NODATA	-	-	-

Table 8: Reclassification of the CLC categories.

1. Urban	**2. Agricultural land**
Continuous urban fabric	Nonirrigated arable land
Discontinuous urban fabric	Permanently irrigated land
Industrial or commercial units	Rice fields
Road and rail networks and associated land	Vineyards
Port areas	Fruit trees and berry plantations
Airports	Olive groves
Mineral extraction sites	Pastures
Dump sites	Annual crops associated with permanent crops
Construction sites	Complex cultivation patterns
Green urban areas Sport and leisure facilities	Land principally occupied by agriculture with significant areas of natural vegetation

3. Forest	**4. Coniferous forest**
Agroforestry areas	Coniferous forest
Broadleaved forest	
Mixed forest	

5. Grassland & Heathland	**6. Shrub**
Natural grasslands	Sclerophyllous vegetation
Moors and heathland	Transitional woodlandshrub
Salt marshes	

7. Marshes & Peatbogs	**8. Other LULCC**
Inland marshes	Beaches dunes sands
Peat bogs	Bare rocks
	Sparsely vegetated areas
	Burnt areas
	Glaciers and perpetual snow

9. Water	**10. No Data**
Salines	No Data
Intertidal flats	
Water courses	
Water bodies	
Coastal lagoons	
Estuaries	
Sea and ocean	

Table 9: Meteorological Stations and their respective Location.

ID	Station	Longitude	Latitude
114140	Älvdalen A	14.0355	61.2536
161910	Älvsbyn A	21.062	65.6691
106570	Åmot A	16.4279	60.9614
159880	Arvidsjaur A	19.2642	65.5941
123460	Börtnan A	13.8427	62.7548
157870	Buresjön A	17.8554	65.558
94390	Daglösen A	14.1803	59.6612
123060	Dravagen A	13.6086	62.0936
115220	Edsbyn A	15.7144	61.3607
148040	Fredrika A	18.3619	64.0744
107420	Gävle A	17.1607	60.7161
155790	Gielas A	15.0645	65.3269
76420	Gladhammar A	16.4526	57.7068
71420	Göteborg A	11.9924	57.7156
145130	Gubbhögen A	15.5529	64.2172
103100	Gustavsfors A	13.799	60.1533
74180	Hagshult Mo	14.1399	57.2926
135460	Hallhåxåsen A	15.3279	63.7685
62040	Helsingborg A	12.7653	56.0304
53530	Hörby A	13.6662	55.8633
146050	Hoting A	16.2356	64.0875
125440	Hunge A	15.0845	62.7504
112540	Idre Fjäll A	12.8521	61.8886
106160	Kerstinbo A	16.9738	60.2683
85460	Kettstaka A	15.0271	58.7162
94190	Kilsbergen-Suttarboda A	14.8956	59.2996
86420	Kolmården-Strömsfors A	16.3069	58.6892
65510	Kosta Mo	15.47	56.8403
136090	Krångede A	16.1699	63.1512
82360	Kroppefjäll-Granan A	12.1973	58.6065
171790	Lakaträsk A	21.1285	66.2789
63510	Ljungby A	13.8794	56.8525
148330	Lycksele A	18.713	64.5481
52350	Malmö A	13.0708	55.5715
104580	Mora A	14.5041	60.9601
191910	Naimakka A	21.5229	68.6762
170930	Nattavaara A	20.9238	66.7516
179960	Nikkaluokta A	19.0212	67.8527
149560	Norsjö A	19.3744	64.9253
95130	Örebro Flygplats	15.0455	59.2289
172940	Paharova A	22.3315	66.8094

182910	Parkalompolo A	22.8219	67.7301
149340	Petisträsk A	19.6943	64.5659
73480	Rångedala A	13.1642	57.7846
65160	Ronneby-Bredåkra	15.2742	56.2619
182810	Saittarova A	22.2288	67.3363
96560	Sala A	16.6843	59.9093
82260	Såtenäs	12.7075	58.4358
105220	Stora Spånsberget A	15.1374	60.3817
93520	Sunne A	13.1166	59.8639
122260	Tännäs A	12.6676	62.4494
126290	Torpshammar A	16.2774	62.4943
97100	Tullinge A	17.9093	59.1785
138070	Västmarkum A	18.2518	63.1243
64510	Växjö A	14.8296	56.8463
160970	Vidsel Mo	20.1543	65.8769
146350	Vilhelmina A	16.8386	64.5798
78400	Visby Flygplats	18.3428	57.6614
173900	Ylinenjärvi A	23.4635	66.6223